Interreg CENTRAL EUROPE

Co-funded by the European Union

TRANSGEO

Feasibility study for the pilot site Zagreb-Savica (Pannonian Basin)

TRANSGEO Deliverable 2.3.5

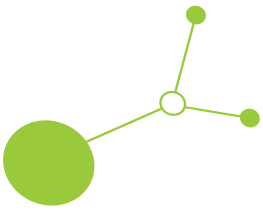

Version 1

10 2025

D2.3.5 Feasibility study for the pilot site Zagreb-Savica (Pannonian Basin)

Corresponding author			
Tomislav Kurevija	University of Zagreb – Faculty of Mining, Geology and Petroleum Engineering (UNIZG – RGNF)	tomislav.kurevija@rgn.unizg.hr	Croatia
Contributing authors			
Luka Perković	University of Zagreb – Faculty of Mining, Geology and Petroleum Engineering (UNIZG – RGNF)	luka.perkovic@rgn.unizg.hr	Croatia
Tomislav Kurevija	University of Zagreb – Faculty of Mining, Geology and Petroleum Engineering (UNIZG – RGNF)	tomislav.kurevija@rgn.unizg.hr	Croatia
Marija Macenić	University of Zagreb – Faculty of Mining, Geology and Petroleum Engineering (UNIZG – RGNF)	marija.macenic@rgn.unizg.hr	Croatia
Katarina Marojević	University of Zagreb – Faculty of Mining, Geology and Petroleum Engineering (UNIZG – RGNF)	katarina.marojevic@rgn.unizg.hr	Croatia
Daria Karasalihović Sedlar	University of Zagreb – Faculty of Mining, Geology and Petroleum Engineering (UNIZG – RGNF)	daria.karasalihovic-sedlar@rgn.unizg.hr	Croatia
Ivan Smajla	University of Zagreb – Faculty of Mining, Geology and Petroleum Engineering (UNIZG – RGNF)	ivan.smajla@rgn.unizg.hr	Croatia

Table of Contents

List of tables

List of figures

0. Executive Summary

This report was prepared within the framework of the TRANSGEO project (https://www.interreg-central.eu/projects/transgeo/). The overall objective of TRANSGEO is to investigate the potential to transform abandoned hydrocarbon wells into new sources of green geothermal energy. To reach this goal, the TRANSGEO team is providing new tools and knowledge to support communities and industries in the energy transition and to break down economic and technical barriers to well reuse. TRANSGEO is co-funded by the European Regional Development Fund through the Interreg Central Europe program.

The main objective of this study is the repurposing of the existing Savica-1 well for geothermal energy use as a Borehole Thermal Energy Storage (BTES) system. The Savica-1 well is located in the southeastern part of the City of Zagreb, within the Peščenica–Žitnjak district. It is close to the industrial zone and the TE-TO Zagreb (combined heat and power plant), which offers favourable conditions for future integration with the city's district heating network. The well was drilled in 1981 with the primary goal of improving a geological understanding of the Zagreb Geothermal Field. The drilling was intended to penetrate the complete Tertiary succession down to its basement since previous wells in this part of the Pannonian basin had not reached a full stratigraphic sequence. Although the original exploration goal was only partially achieved at that time, geological, geophysical, and thermal data were obtained, which confirm the presence of lithothamnion limestones and breccia-conglomerates with temperatures up to 94.4 °C. Because of its low brine production capacity and its location within the city's industrial zone, close to the TE-TO Zagreb, the Savica-1 well was selected as a pilot site for Borehole Thermal Energy Storage. To assess the feasibility of repurposing the well, a numerical modeling framework was developed with a Python-Feflow interface.

The report reflects the views of the authors.

1. Introduction

As a transition towards 4th generation district heating and decarbonized heating, BTES solutions are being widely introduced, especially for older existing wells which have potential to be revitalized. As part of TRANSGEO project activities, this feasibility study should examine the conversion of the 2.2 km deep abandoned well into a Borehole Thermal Energy Storage (BTES) system. It is an ideal pilot for storage of waste heat in BTES, due to its location in an industrial heat demand zone of Zagreb near an existing cogeneration power plant, where summer waste heat is available as an energy source for BTES.

To facilitate future investment at this site, as part of this study, it is necessary to model framework of BTES system based on transient simulation of energy balance flows in the surface equipment, similar to deep borehole heat exchanger (DBHE), and the simulation of heat transfer in geothermal reservoir. The simulation needs to be in a coupled approach for all three system components modelled by separate balance equations. The modelling framework for the BTES/DBHE needs to be built on 1D energy balance for coaxial BHE with annular inlet (CXA exchanger – coaxial annular inlet). The modelling framework for the geothermal reservoir is finite element analysis (FEM). Both BHE and reservoir modelling approach are done in a commercially available software, FeFlow. Surface equipment is modelled with user-defined scripts in which all model features are combined with a set of specific equations describing each component. The full coupling is done with a Python-Feflow interface.

The framework is tested on a hypothetical case study for a single-well BHE (acting as a single-well deep BTES) integrated into a district heating (DH) network of the city of Zagreb. During the winter period, the DH is supplied directly from the BHE and industrial waste heat, where BHE is used first. During the summer period industry is rejecting the excess heat due to limited flexibility. In combination with this waste heat and lack of thermal demand, the BHE could now be used to reject the heat into the reservoir to enhance its thermal recovery before the new heating season starts.

Therefore, this Study will give a good foundation for future investment into BTES at Savica site. Also, results of this Study can be easily implemented for any other BTE system with different initial setup.

2. Geographic Location and Analysis of Spatial Planning Documentation

2.1. Location

The Savica-1 well is located in the city district of Peščenica – Žitnjak, within the administrative-territorial unit of the City of Zagreb (Figure 1), at the following coordinates:

- Y (northing): 5,581,255.20
- X (easting): 5,071,245.03
- Elevation (H): 109.74 meters above sea level

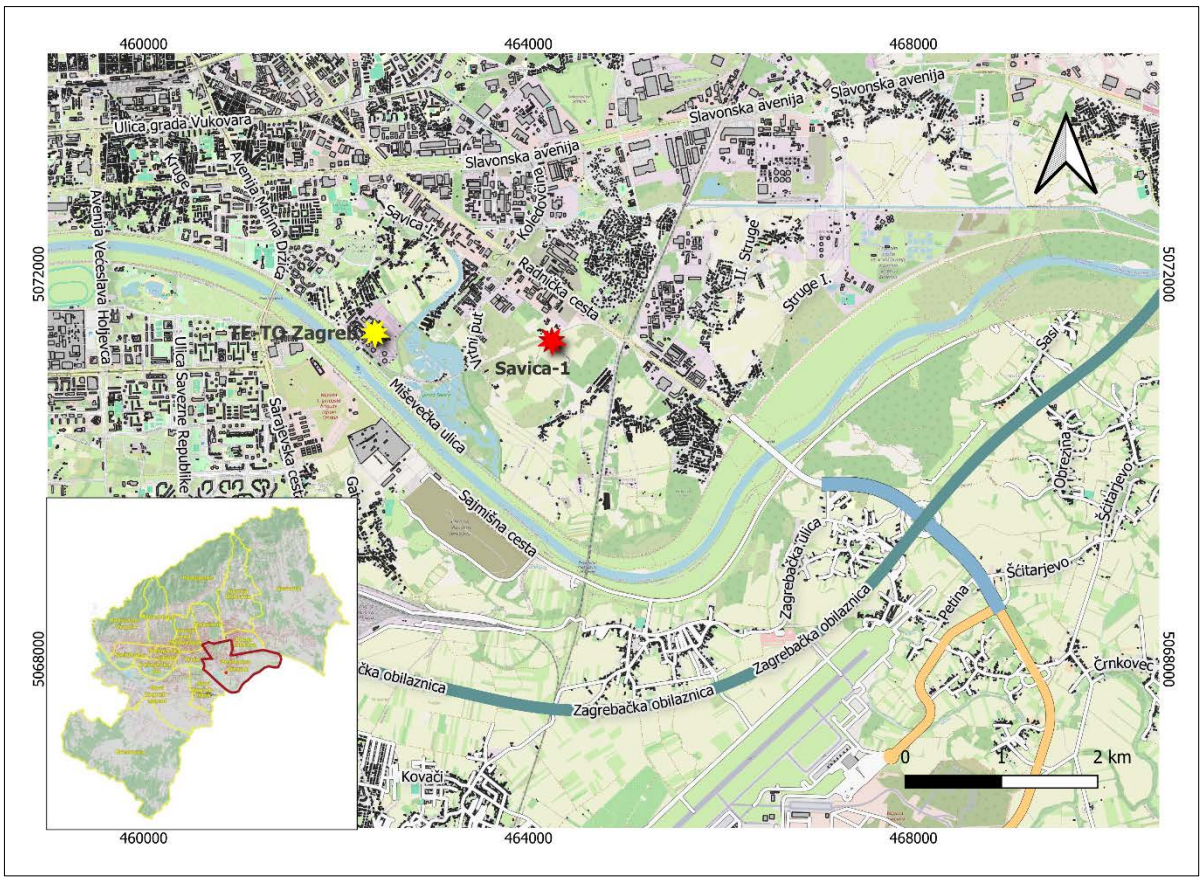

Figure 2.1. Savica-1 well location

The Peščenica-Žitnjak city district encompasses the southeastern part Zagreb and within its boundaries is the independent settlement of Ivanja Reka. The northern part (Peščenica) is bordered by Heinzelova Street, extending north to Zvonimirova Street. The southern part lies east of Držićeva Avenue, south of Slavonska Avenue, and north of the Sava River. The district includes quarters: Volovčica, Borongaj, Ferenščica, Borovje, Savica Šanci, Folnegovićevo Naselje, Petruševec, Struge, Kozari Putevi, Kozari Bok, Vukomerec, Resnik, and Ivanja Reka. The district spans an area of 35.26 km^2 and has a population of 53 023 (2021). In addition, the Zagreb Combined Heat and Power Plant (TE-TO Zagreb) is located within this district, marked on the map with a yellow star.

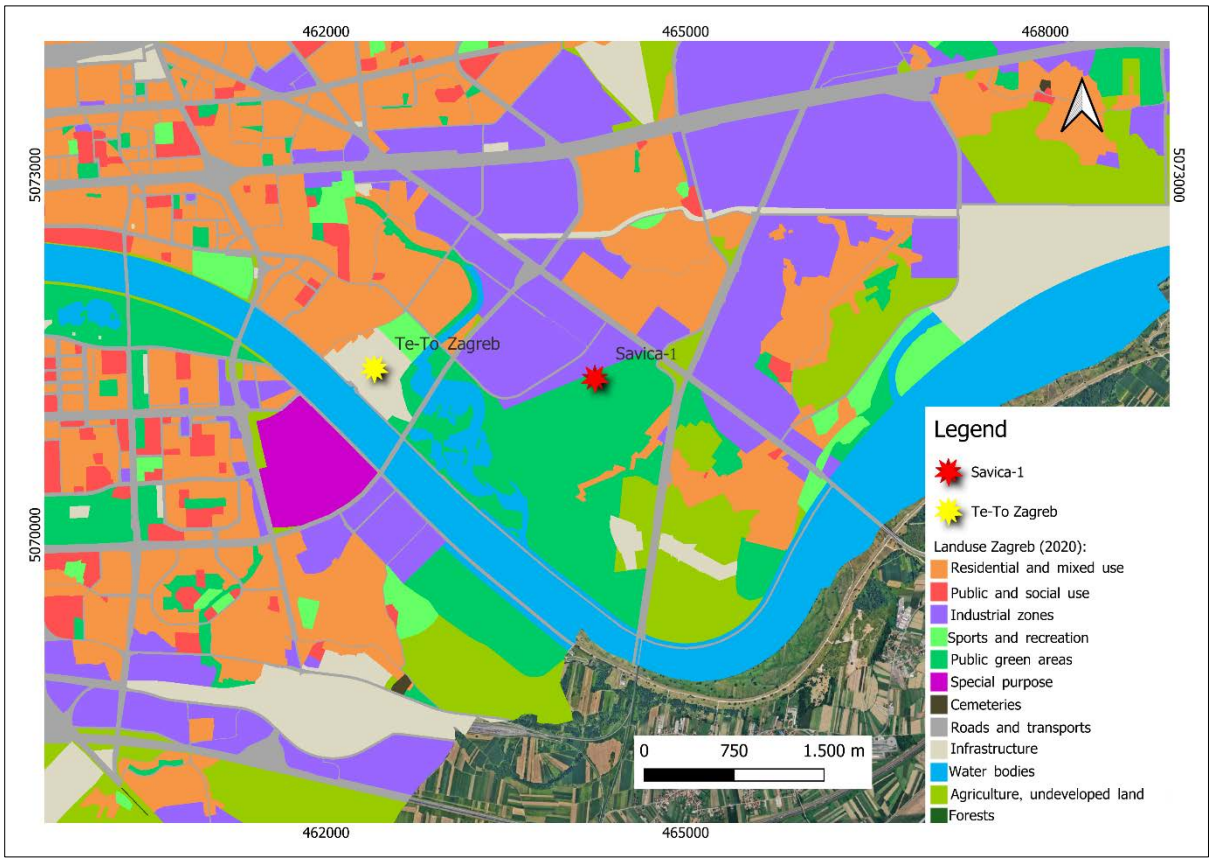

Figure 2.2. Actual Land Use of the City of Zagreb 2020. Base map source: Geoportal DGU

Regarding the Savica-1 well itself, it is located within an industrial zone, approximately 2 kilometers north of the Sava River channel. South of the well, there are cultivated agricultural areas, while to the west lies a group of small lakes, remnants of former Sava meanders and gravel pits. The surrounding industrial area hosts a range of facilities, including the Graphic Institute of Croatia, Telecommunications service provider - A1 Hrvatska d.o.o., an INA warehouse, Zagreb Printing House, Metal i Staklo d.o.o., and many others. Given the concentration of industrial and commercial facilities, the entire business complex presents significant potential for the utilization of geothermal energy from the Savica-1 well. Figure 2 shows the land use map of Zagreb (2020). Different land use categories are represented by colors, including industrial zones, mixed-use areas, transport corridors, green areas, and water bodies.

2.2. Transport Connectivity

The Peščenica-Žitnjak city district is well-integrated into Zagreb's public transportation and road infrastructure. The district is primarily serviced by the city's tram and bus network, operated by The Zagreb Electric Tram (ZET) (Croatian: Zagrebački električni tramvaj), providing direct connectivity to central and eastern parts of the city. An important infrastructure feature in the area is the Homeland Bridge (Croatian: Domovinski most), an 840-meter-long structure over the Sava River that accommodates four lanes of vehicular traffic and space for future railway tracks. This bridge directly links Radnička Street in the north with the Velika Kosnica and the Zagreb bypass (Croatian: Zagrebačka obilaznica) to the south, serving as a critical transport corridor.

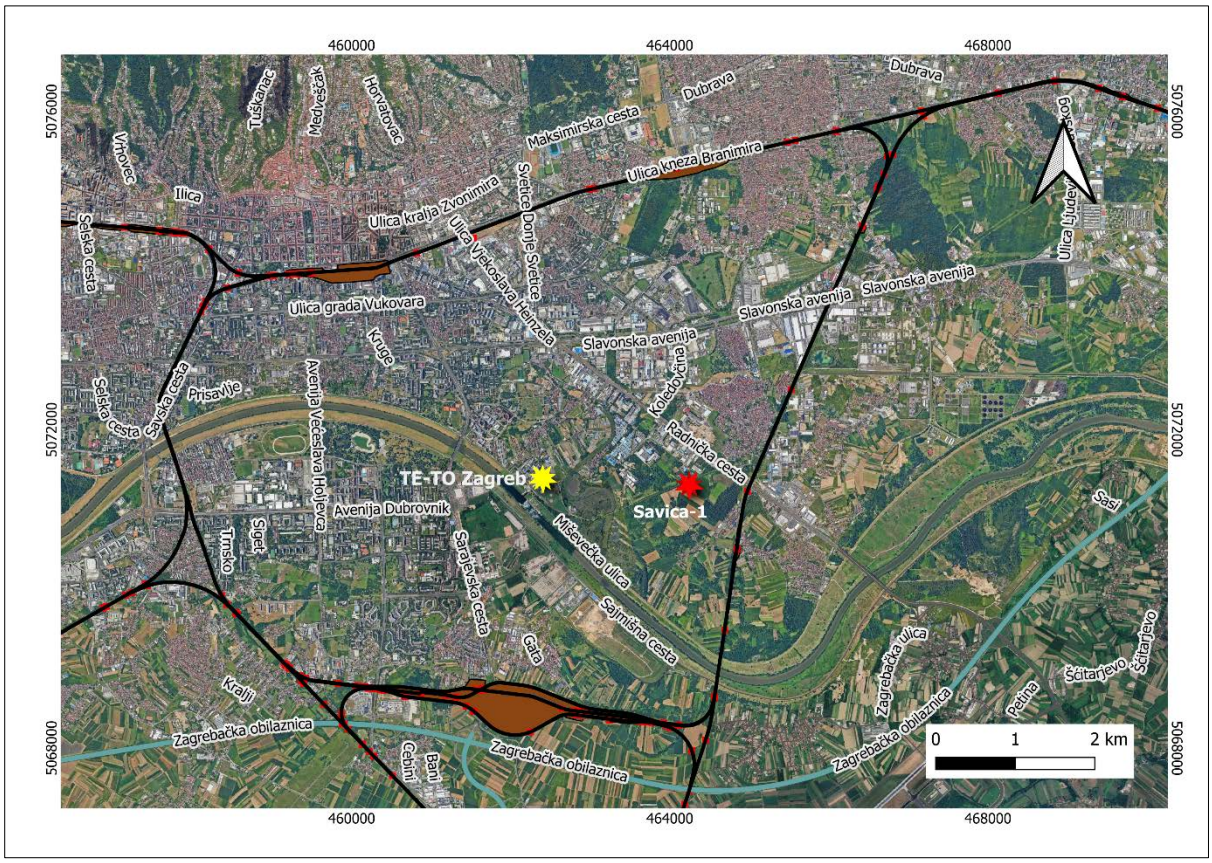

Figure 2.3. Location of TE-TO Zagreb, position of the Savica-1 well and the railway corridor (Infrastrukturni pojas HŽ Infrastrukture d.o.o. - WMS INSPIRE)

Radnička cesta functions as one of the main radial roads, connecting the city center to Peščenica – Žitnjak and further toward the southern and eastern periphery. Sajmišna cesta, located further to the south, serves as an important local and regional connector road, facilitating access to the Zagrebački velesajam (Zagreb Fair), Homeland Bridge, and surrounding industrial zones. The district also benefits from good accessibility to the A1, A3, and A4 motorways, making it strategically important for regional transport and logistics. Additionally, Franjo Tuđman International Airport is located approximately 10 km southeast of the district, allowing for quick access to air transport. Figure 3 illustrates the location of TE-TO Zagreb, the Savica-1 well, the nearby railway corridor that could serve as a potential route for district heating pipelines, as well as major access roads that provide vital connections within the district and toward the wider Zagreb area.

2.3. Power Grid

Zagreb's electricity supply is part of the national transmission system managed by HOPS, Croatian Transmission System Operator Plc., a subsidiary of HEP Group Croatian electro energetic company. Zagreb's electricity supply is primarily secured via the Žerjavinec, Tumbri and Mraclin substations (Figure 4), which are key nodes in the 400/220/110 kV and 110 kV transmission network. According to the 110 kV grid scheme of the Zagreb transmission area, the city is embedded in a dense and well-connected infrastructure comprising both overhead lines and cable routes. Table 1 provides a detailed overview of Zagreb's transmission network, including the total length of overhead lines and cables, the number of substations, switchgear fields, transformers, and the installed capacity. Figure 5 illustrates electricity transmission lines within the broader area of investigation.

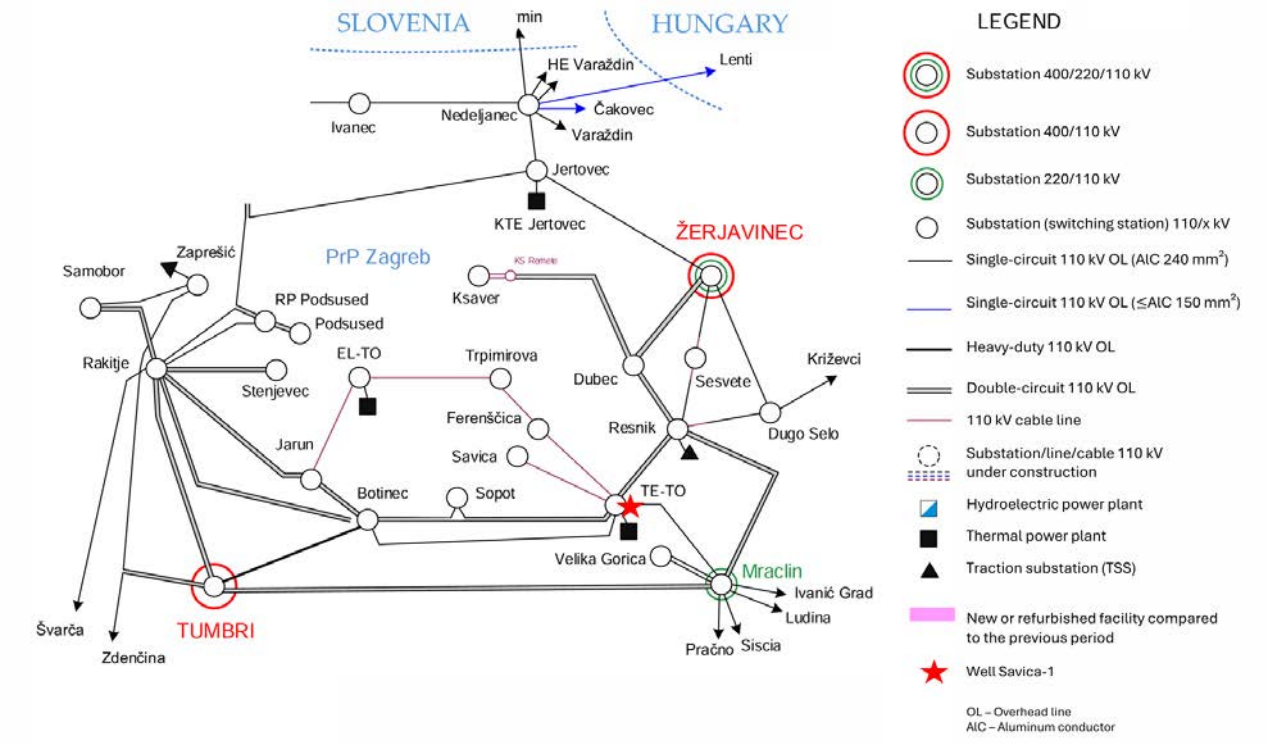

Figure 2.4. Zagreb electricity supply (HOPS)

Voltage Level (kV)	Length of Overhead Lines and Cables (km)	Number of Substations	Number of Switchgear Fields	Number of Transformers	Installed Capacity (MVA)
400 kV	527.83	2	18	6	1 900
220 kV	415.60	4	27	4	750
110 kV	1,833.00	60	384	51	1 521.5
Submarine / Underground (s.n.)	0.00	-	-	-	-
Total	2,776.43	66	429	61	4 171.5

Table 1. Transmission Network – City of Zagreb (as of 31 December 2023)

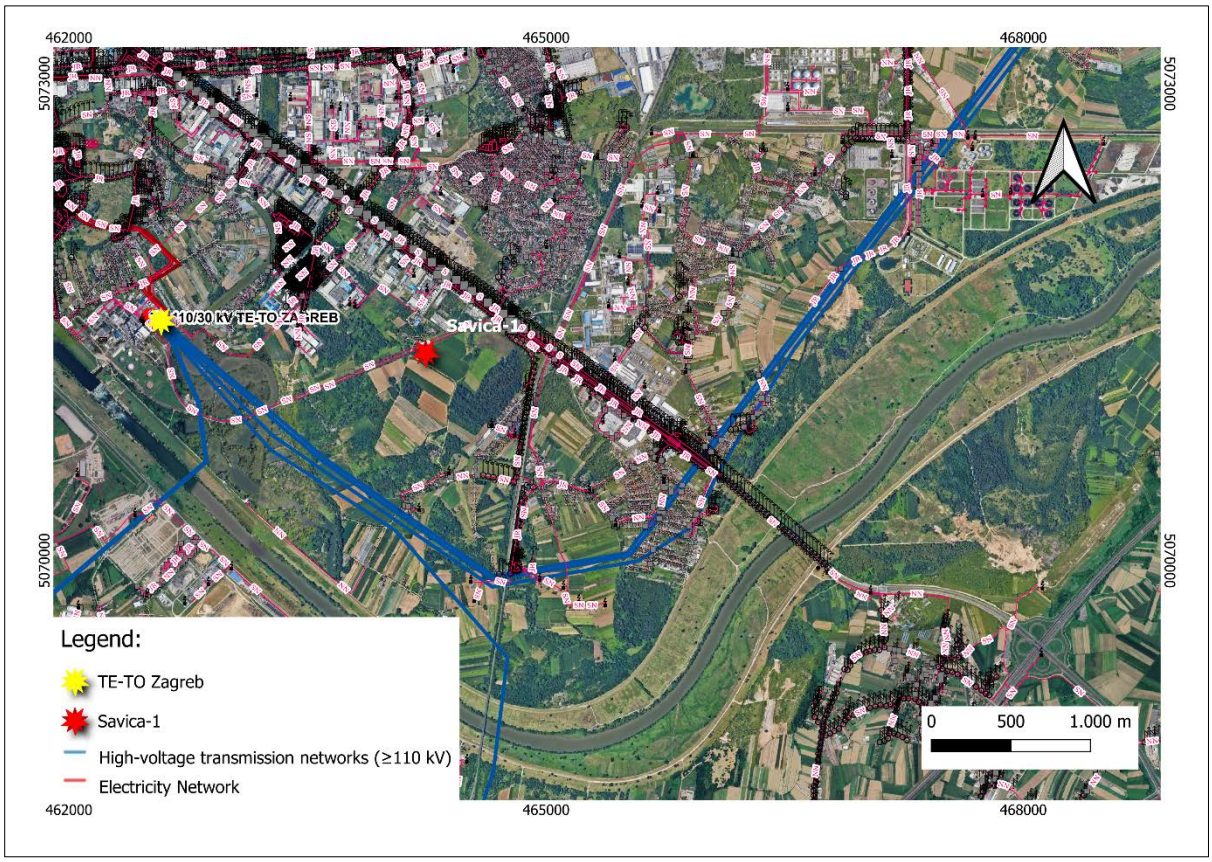

Figure 2.5. Electricity transmission lines within the broader area of investigation (ZG GEOPORTAL)

2.4. Demographic Aspects

The location of the Peščenica – Žitnjak district, within the administrative-territorial unit of the City of Zagreb, is positioned in the eastern part of the capital. It encompasses both residential and industrial zones, making it an area of mixed urban and economic function. According to the most recent demographic data, the district has a total of 53,023 inhabitants, with a slightly female-majority population (53.2% women, 46.8% men) (Figure 6). The age distribution indicates a relatively balanced structure, with a high concentration of population in the working-age groups (25–44 years), particularly those aged 30–39, which together account for the largest share of residents. The population concentration map shows that the highest density of residents is in the western and central parts of the district, while the eastern and southern segments are less densely populated (Figure 6).

In terms of population aging, the number of inhabitants steadily decreases after the age of 65, with a significantly lower share in the 85+ category (Figure 7). The presence of 2,867 children aged 0–4 indicates ongoing, albeit moderate, population renewal.

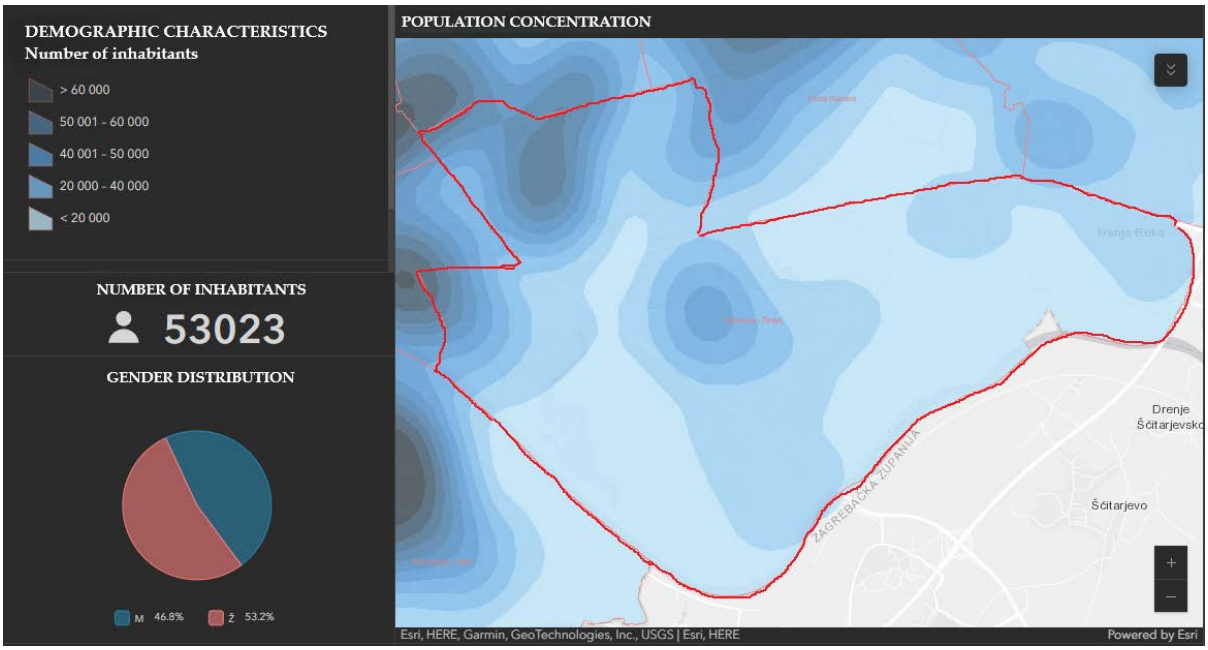

Figure 2.6. Population concentration (https://arcg.is/0z9bKi)

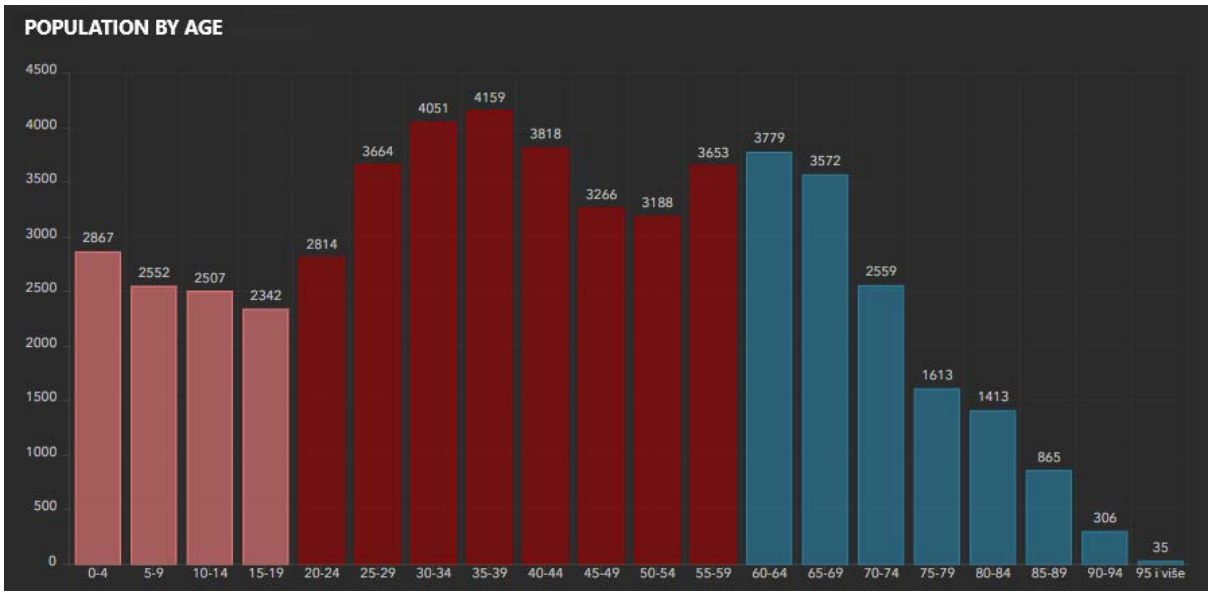

Figure 2.7. Population by age (https://arcg.is/0z9bKi)

2.5. Compliance of Interventions with Current Spatial Planning Documentation

2.5.1. Spatial Plan of the specific site of the well Savica-1

General Urban Plan of the City of Zagreb (Official Gazette of the City of Zagreb Nos. 16/07, 8/09, 7/13, 9/16, 17/24 – consolidated text established by Official Gazette of the City of Zagreb No. 15/23)

6.5. Energy System

Article 50

The General Urban Plan defines areas and corridors for the development of the energy system for:

- *electricity;*
- *thermal energy;*
- *natural gas.*

Existing and planned energy system structures and networks are shown on cartographic representation 3. TRAFFIC AND UTILITY INFRASTRUCTURE NETWORK – 3b Energy system, postal and telecommunications. The symbols used in the cartographic representations indicate approximate locations.

According to Article 27 of the Decision on Amendments to the Decision on the Adoption of the General Urban Plan of the City of Zagreb (Official Gazette of the City of Zagreb 8/09), a sentence was added at the end of paragraph 2.

Facilities and structures for the use of renewable energy sources may be installed in accordance with the urban rules of this decision and professional standards in all land-use zones.

According to Article 26 of the Decision on Amendments to the Decision on the Adoption of the General Urban Plan of the City of Zagreb (Official Gazette of the City of Zagreb 7/13), a new paragraph 3 was added after paragraph 2.

6.5.2. Structures for the Supply of Thermal Energy

Article 52

The supply and use of thermal energy in the city shall be ensured through appropriate land use and the designation of corridors for:

- *extension of the distribution network;*
- *interconnection of TE-TO and EL-TO networks;*
- *construction of pumping stations;*
- *installation of steam pipelines underground;*
- *construction of new buildings at TE-TO and EL-TO sites;*
- *use of geothermal energy;*
- *construction of structures for the passive use of solar energy, wind energy, and biogas;*

According to Article 29 of the Decision on Amendments (Official Gazette 8/09), in paragraph 1, at the end of the 7th bullet point, the full stop was replaced with a comma, and the words "wind energy and biogas " were added.

- *use of energy from future waste-to-energy plants;*
- *in areas where CTS exists or is planned together with other energy sources, the energy source more acceptable to consumers shall be used.*

The distribution network of the central heating system (hot water and steam pipelines) shall be laid underground in accordance with special regulations.

The required corridor for laying the distribution network of the central heating system (hot water and steam pipelines), depending on the pipeline profile, ranges from 2 m to 4 m.

Exceptionally, the reconstruction and parts of the new distribution network of the central heating system (hot water and steam pipelines) may be laid, depending on local technical conditions, on all types of land use, in accordance with Articles 22 and 56 of this decision.

According to Article 26 of the Decision on Amendments (Official Gazette 9/16), new paragraphs 2, 3, and 4 were added after paragraph 1.

Provided they do not negatively affect the surroundings, the construction and installation of devices for the use of solar energy is permitted, taking into account restrictions related to MEASURES FOR THE PRESERVATION AND PROTECTION OF LANDSCAPE AND NATURAL VALUES AND IMMOVABLE CULTURAL HERITAGE.

According to Article 28 of the Decision on Amendments (Official Gazette 7/13), a new paragraph 2 was added after paragraph 1.

According to Article 26 of the Decision on Amendments (Official Gazette 9/16), the previous paragraph 2 became paragraph 5.

URBAN RULES

8.1. General Provisions

Article 56

Urban rules are defined in accordance with natural and urban-architectural heritage, local conditions, the level of area consolidation, and land use and function.

According to spatial planning criteria and the stability of the urban matrix, three levels of consolidation are distinguished:

- *highly consolidated areas;*
- *consolidated areas;*
- *low consolidated areas.*

Urban rules define spatial arrangement requirements and location conditions for construction, except in areas designated as city projects.

Urban rules are shown in cartographic representation 4. CONDITIONS FOR LAND USE, ARRANGEMENT, AND PROTECTION OF SPACE – 4a Urban Rules.

In land-use zones Z, Z1, and Z2 that are not specifically categorized by urban rules, the provisions of Articles 66, 67, 78, and 79 of this decision shall apply depending on the level of consolidation. In areas designated as R1, R2, IS, and cemeteries not specifically categorized, Article 77 applies.

Construction is not permitted on forested land, except for infrastructure and structures serving forestry purposes, in accordance with the Forest Act and the Nature Protection Act. Exceptionally, the expansion of the Urn Grove is permitted under special conditions.

The construction and installation of devices for the use of renewable energy sources is permitted, provided they do not negatively affect residential quality and considering restrictions related to MEASURES FOR THE PRESERVATION AND PROTECTION OF LANDSCAPE AND NATURAL VALUES AND IMMOVABLE CULTURAL HERITAGE.

...

In the urban development plan, when planning new residential or mixed-use neighborhoods, the use of renewable energy sources must be ensured in accordance with professional standards, as well as at least a

minimum standard of supporting facilities, including a square, playground, park area, and connection to the city's transportation network proportionate to the number of users of that space.

Article 87

A1 PROTECTED AREAS UNDER THE NATURE PROTECTION ACT WITHIN THE PLAN AREA

SIGNIFICANT LANDSCAPE

A significant landscape is a natural or cultivated area of high landscape value and biodiversity and/or geodiversity, or a landscape that preserves the unique characteristics typical of a particular area.

In a significant landscape, only interventions and activities that do not compromise the values for which it was designated are permitted.

Within and near designated significant landscapes, interventions and actions that may negatively affect habitat conditions and the stability of plant and/or animal populations are not acceptable. These include: intensive logging; construction of power plants (including those using renewable energy sources); mineral resource extraction; hydraulic engineering works and land reclamation; land-use conversion; construction of golf courses; installation of antenna masts; contamination of surface and groundwater; and introduction of alien (non-native) species.

MEASURES TO PREVENT ADVERSE ENVIRONMENTAL IMPACT

Article 98

In the area of the City of Zagreb, no development of activities that endanger human health or harm the environment is foreseen.

Measures to reduce and prevent adverse environmental impacts:

…

The water source protection area is divided into three protection zones for which protection guidelines are prescribed:

Zone I – strict protection and monitoring

…

Zone II – restricted protection and monitoring:

In Zone II, the following is prohibited:

…

subsurface and surface extraction of mineral resources, except for geothermal and mineral water,

…

drilling of exploration and production wells, except those related to public water supply and renewable energy sources

…

Zone III – limitation and monitoring

In Zone III, the following is prohibited:

…

subsurface and surface extraction of mineral resources, except for geothermal and mineral water.

3.Research Area of well Savica-1

3.1. General Description

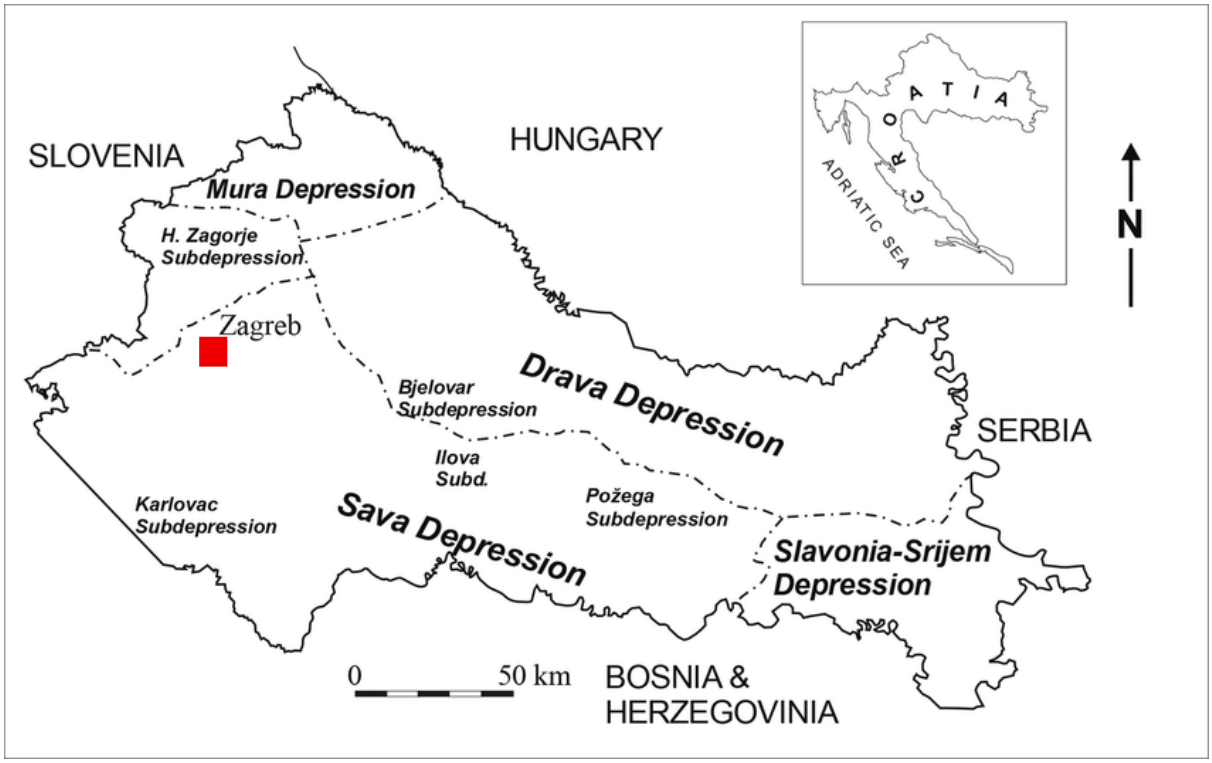

Figure 3.1. Neogene-Quaternary depressions in the Croatian part of the Pannonian Basin System (Malvić, 2016)

The Croatian part of the Pannonian Basin System (CPBS) approximately covers the northern part of Croatia over an area of about 20,000 km². It is divided into four Neogene–Quaternary depressions: the Drava, Sava, Mura, and Slavonija–Srijem (Malvić, 2016). The well Savica-1 is located in the city of Zagreb (marked in red), in the northwestern part of the Sava Depression (Figure 8).

Subsurface structure of the Sava depression is known from drilling data and numerous geophysical surveys conducted in connection with petroleum geological exploration in this area. Its shallower and surface parts have been analyzed through hydrogeological investigations and surface geological mapping. The depression is characterized by the development of a thick series of Neogene sediments, which in many locations exceed 3,000 m in thickness. This considerable thickness is the result of movements along marginal faults, accompanied by intense subsidence of the Sava basin relative to its surrounding uplifted margins (Basch, 1983).

During the Late Pannonian and Early Pontian (9.3–5.6 Ma), and in some areas already from the Early Pannonian, depressions within the CPBS developed into elongated brackish lakes (Malvić and Velić, 2011), which were sporadically interconnected by narrow channels (Figure 9). These depressions originated from Lake Pannon (Magyar et al., 1999), an extensive lacustrine system that formed following the closure of the Central Paratethys (Royden, 1988). Sedimentation in the Croatian brackish lakes is predominantly characterized by heterogeneous deposition of two main lithofacies, with the Eastern Alps serving as the principal source of psammitic detritus. Continuous hemipelagic (pelitic) sedimentation of calcite muds and

clays was periodically interrupted by the deposition of medium- to fine-grained sands transported by turbidity currents (Vrbanac et al., 2010).

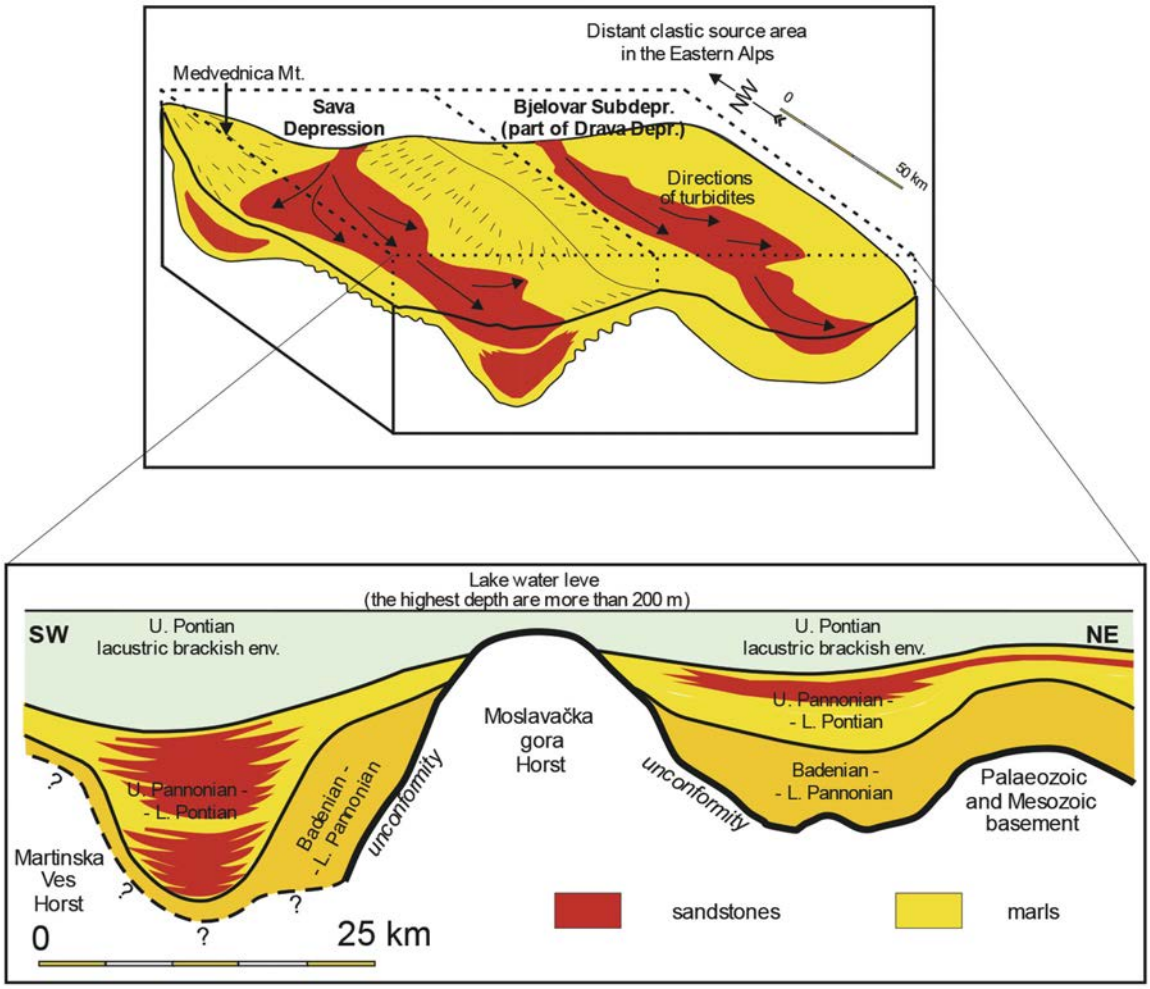

Figure 3.2. Schematic review of depositional environments, recent sediments and palaeo-directions of turbidites during Upper Pontian in the CPBS (After Vrbanac et al. (2010), modified in Malvić (2016))

The Neogene and Quaternary sedimentary complexes are divided into three major megacycles (Velić et al, 2002).

The oldest, first megacycle, corresponds to the Prečec Formation of Badenian and Sarmatian age (and locally also Early Miocene). It comprises highly heterogeneous lithologies, including breccias, conglomerates, sandstones, siltstones, shales, marls, igneous rocks, and limestones. The second megacycle, assigned to the Pannonian and Pontian stages, encompasses the Prkos, Ivanić-Grad, Kloštar Ivanić, and Široko Polje Formations, characterized by monotonous alternations of marlstone and sandstone sequences. The third megacycle, represented by the Lonja Formation of Pliocene and Quaternary age, predominantly consists of unconsolidated sediments such as sands, gravels, loess, and locally lignite. The main oil and gas reservoirs in the region are found within the sandstones of the second megacycle. The formations described above are shown in Figure 10.

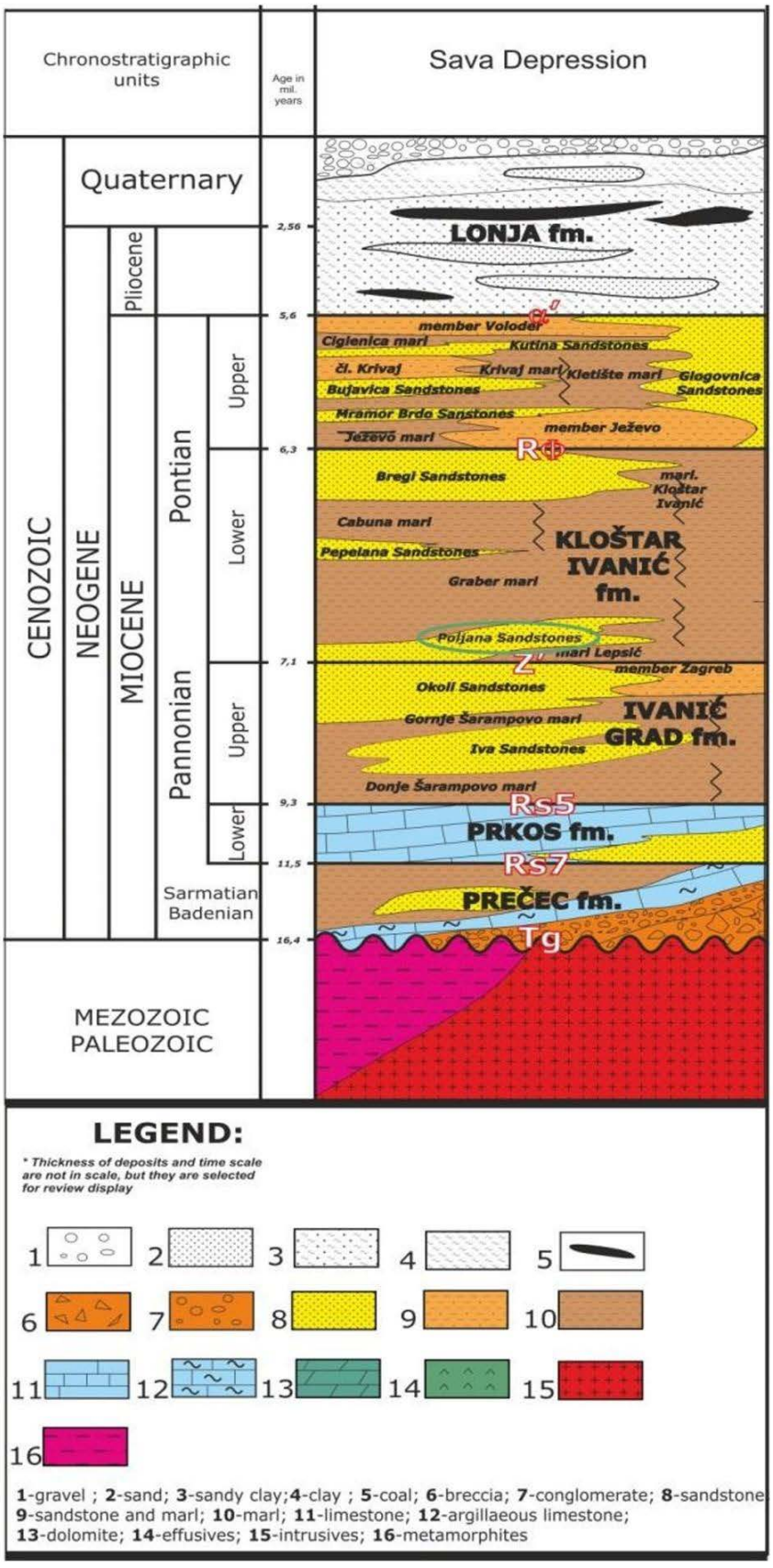

Figure 3.3. Chronostratigraphic and lithostratigraphic units in the Sava Depression (Podbojec and Cvetković, 2015)

3.2. Zagreb geothermal field

The exploitation field “Geothermal Field Zagreb" covers an area of 54 km² (9 km × 6 km) and is administratively located almost entirely within the City of Zagreb, while a small part (slightly more than 2.5 km²) lies in Zagreb County, in the municipality of Stupnik (Lučanka-1 well) (Figure 11). The field boundaries largely extend across the area of the City of Zagreb and to a smaller extent across the settlements of Lučko, Hrvatski Leskovac, Gornji Čehi, Botinec and Donji Stupnik. The area where the field is located lies on slightly inclined terrain, from the west (125 m a.s.l.) and southwest (130 m a.s.l.) towards the east of the field (112.5 m a.s.l.) Within the exploitation field, there are 15 wells, of which three are production, two are injection, eight are monitoring, and two are abandoned (Table 2).

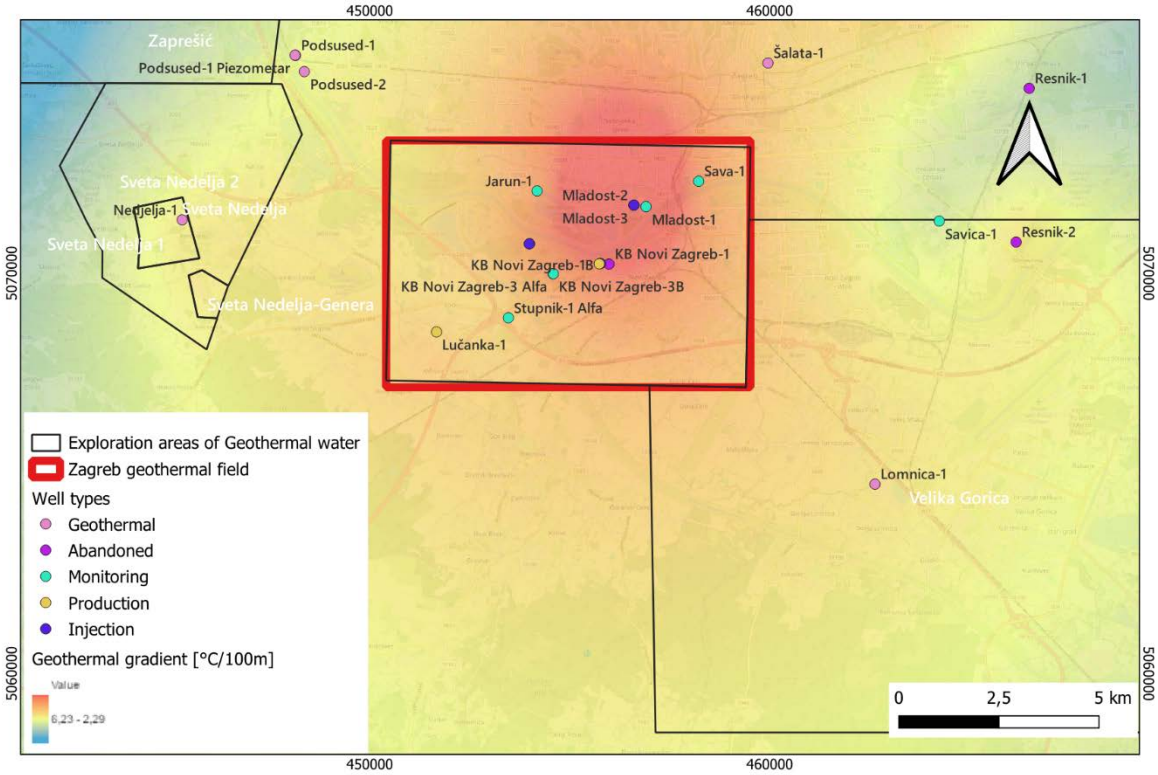

Figure 3.4. Location of wells within the Zagreb geothermal field and surrounding exploration areas

Well type	Well name
Production	Mladost-3, KB Novi Zagreb-1B, Lučanka-1
Injection	Mladost-2, KB Novi Zagreb-1A
Monitoring	Mladost-1, KB Novi Zagreb-2, KB Novi Zagreb-2A, KB Novi Zagreb-3α, KB Novi Zagreb-3B, Sava-1, Jarun-1, Stupnik-1α
Abandoned	KB Novi Zagreb-3, Stupnik-1

Table 2. Classification of wells within the Zagreb geothermal field according to their current operational status.

The reservoir is classified as a massive-type reservoir formed in the dolomites of the Tertiary basement and in Miocene lithothamnion limestones with pronounced vertical permeability. The reservoir rock is characterized by both primary and secondary porosity. The value of the geothermal gradient within the Zagreb geothermal field is variable and ranges between 5.7 and 7.8 °C/100 m, which is higher than the average gradient of the Sava Depression, amounting to 4.8 °C/100 m.

In the Zagreb Geothermal Field, geothermal energy is utilized through two technological systems and one subsystem:

- the technological system „Mladost";
- the technological system „Clinical Hospital Novi Zagreb";
- the technological subsystem at the Lučko site.

Since 1981, only minor quantities of thermal water have been produced, accounting for less than 10% of the potential production capacity of the Zagreb geothermal field. The thermal water is used for heating swimming pools within the Sports and Recreation Center „Mladost," for heating storage facilities within the „Clinical Hospital Novi Zagreb," and for heating buildings at the Lučko site. The reason for such low consumption of thermal water, as already mentioned in the previous report, is primarily the lack of new consumers.

3.2.1. Exploration History of the Zagreb Geothermal Field

The Zagreb Geothermal Field was discovered in 1964 with the negative oil exploration well Stu-1 and subsequently confirmed through hydrodynamic testing in 1977. Interpretation of the boundary test estimated a reservoir volume of 1.157×10^9 m³ of geothermal water, with an average temperature of 57 °C, at depths between 733–815 m. For the interpretation of the field, it was necessary to investigate the wider area using surface geological and geophysical surveys, which were later carried out. According to scope and type, the following investigations were performed: geological mapping covering the entire field area; 589 gravimetric measurements with an average density of 11 points/km² and 389 magnetometric measurements with an average density of 7 points/km²; 20 geoelectrical soundings and 70 km of seismic profiles, of which 58 km (1.1 km/km²) were used for interpretation. In this way, part of the Zagreb geothermal aquifer system was investigated. In the broader sense, it includes permeable deposits extending from Samobor in the west to Resnik in the east and Dubranec in the southeast. The degree of exploration of this relatively large area, however, remains low. Subsequently, the well Mladost-1 was drilled in 1980, and by the end of 1986, an additional 13 wells had been drilled (listed in Table 3).

Year	Wells
1964	Stupnik-1 (Stu-1)
1979	Stupnik-1α (Stu-1α)
1980	Mladost-1
1984	KB Novi Zagreb-1A, KB Novi Zagreb-2, Sava-1
1985	Mladost-2, Mladost-3, KB Novi Zagreb-3, KB Novi Zagreb-3α, KB Novi Zagreb-3B
1986	KB Novi Zagreb-1B, Lučanka-1 (Luč-1), Jarun-1
1988	KB Novi Zagreb-2A

Table 3. Chronological overview of wells drilled within the Zagreb geothermal field

All encountered thermal water-bearing horizons are in Miocene lithothamnion limestones, and some are also in Mesozoic dolomites. Within the exploitation field, all wells except KBNZ-2, KBNZ-3 and KBNZ-3B were included in interference tests. These tests demonstrated that all wells intersect the same unified hydrodynamic unit, regardless of lithological differences.

The Mladost-1 well operated continuously until the end of June 1986 (when new facilities for the 1987 Universiade were built). During winter, the thermal energy was used directly for heating the sports hall without a heat exchanger, while in spring–autumn it was used for heating outdoor swimming pools. Initially, geothermal water was mixed with technical water, but later heating was performed using a heat exchanger.

Well KBNZ-1A was completed in 1984 (the Blato group of wells was drilled to supply heat energy to the facilities of the Clinical Hospital Novi Zagreb – KBNZ). At the end of the same year, it began to be used for heating temporary buildings at the KBNZ construction site through a heat exchanger. By mid-1985, two production wells had produced a total of about 500,000 m^3 of water, accompanied by a reservoir pressure drop of 1.6 bar. From mid-1985 to mid-1986, the remaining wells at the Zagreb Geothermal Field (except KBNZ-2A) were drilled and equipped. During productivity testing of the wells (KBNZ-1B, KBNZ-3α), the total amount of water produced, including the earlier production from KBNZ-1A and KBNZ-2, reached approximately 620,000 m^3. The pressure declines and results obtained from hydrodynamic testing (reservoir limit test) required a change in reservoir management, introducing secondary pressure maintenance by reinjecting geothermal water back into the reservoir.

Reservoir pressure behavior at the Blato site for the period June 1986 – June 1992 showed the following recovery characteristics: a rapid pressure increase between June and October 1986, when the wells were shut-in (following forced production); stabilization of pressure until the end of 1988 through the application of secondary reservoir management methods, followed by a gradual decline until mid-1992.
Well KBNZ-1A remained in use until the end of 2002, operated exclusively during the winter months. Since the beginning of 2003, the production well has been KBNZ-1B, while geothermal water, after passing through a heat exchanger, has been reinjected into the previously productive well KBNZ-1A.

3.2.2. Geological setting of the Zagreb Geothermal Field

Quaternary (Q)

The youngest deposits are Quaternary sediments of various lithologies, dominated by alluvial deposits of the Sava River. These are mostly gravels that represent the main collector used for public water supply in the City of Zagreb, directly connected to the Sava River. The gravels contain sands, sandy clays, loess, humus and are irregular in thickness. These sediments are discontinuous, often exploited in gravel pits (e.g., Jarun, Bundek, Čiče). The geothermal wells were not cored in these intervals, so data on thickness are missing.

Pliocene (Pl)

Composed of clayey-sandy sediments without clear differentiation of sandstone members. Predominantly sandy-clayey deposits, with sandstone layers of poor collector quality, weak permeability, and limited groundwater potential. Classified as aquitard.

Upper Miocene – "Gornji miocen" (M^2–M^1_6)

Overlying the main geothermal aquifer are marl deposits of the Ivanić Grad Formation (Prkos Member). These represent a sealing unit. Locally, sandy intercalations are present but overall hydrogeological properties classify this interval as impermeable.

Middle and Lower Miocene (M_5–M_1)

These sequences comprise biogenic limestones, breccias, and conglomerates of varying thickness. In some wells (Jrn-1, Sava-1), thick breccias were recorded, acting as potential geothermal reservoirs, though the collector quality varies. At depth, biogenic limestones are overlain by impermeable marls and clays, reducing transmissivity. Hydrogeological properties are mixed, with secondary porosity prevailing.

Tertiary (T)

This complex includes carbonate deposits—dolomites and lithothamnion limestones—forming the main geothermal aquifer in the Zagreb area. The unit is well developed in the Samobor and Medvednica Mountains and continues into the geothermal field. It represents the primary reservoir, with dolomites and breccias acting as high-permeability collectors.

Tertiary Basement / Pre-Tertiary (PT)

Below the Tertiary, dolomites and dolomitized limestones with limited thickness are present. In several wells (e.g., Mla-2, KBNZ-3α), the sequence terminates in dolomites that exhibit poor circulation, but in others, they act as permeable horizons. Hydrogeological classification is variable; in places, dolomites form aquifers, in other aquitards.

Basement ("Temeljno gorje", Tg)

The deepest rocks encountered are of pre-Tertiary age: gneisses, schists, and low-grade metamorphic rocks of the Medvednica Massif. These rocks are impermeable and do not function as aquifers.

3.3. Well Savica-1

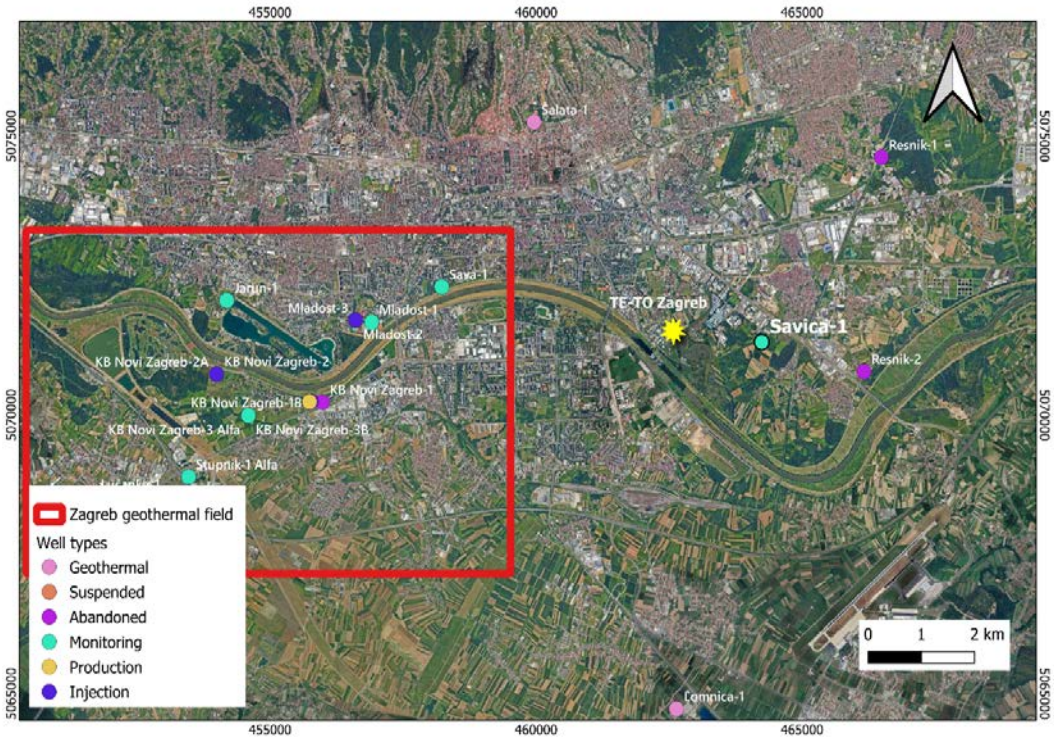

Figure 3.5. Location of the Savica-1 well and TE-TO Zagreb in relation to the Zagreb geothermal field and surrounding wells

To improve understanding of the aquifer in the southeastern part of the Zagreb area, the exploratory well Savica-1 was drilled on September 8, 1981. Its location was selected based on data obtained from earlier oil and gas exploration wells, which had already indicated the presence of warm water-bearing formations. The well is situated southeast of the city, on the left bank of the Sava River, within the Žitnjak horticultural complex and next to the industrial railway track of the Resnik Heating Plant. The drilling target was set at 2120 m, to penetrate the complete Tertiary succession down to its basement, since previous wells in this part of the basin had not reached the full stratigraphic sequence. The well has the status of a monitoring well (Figure 12). Figure 13 shows the Savica-1 wellhead, with no surface equipment installed and only a concrete platform marking its location.

Figure 3.6. Savica-1 wellhead

3.3.1. Well Construction Savica-1

The total depth of the Savica-1 borehole is 2022.2 meters.

Casing (Figure 3.5):

- Surface casing (13 3/8") installed to 122.7 m and cemented to the surface.
- Ⅰ Intermediate casing (9 ⅝") installed to 618.7 m and cemented to the surface.
- Ⅱ Intermediate casing (7") installed to 1247 m.

Details of the well construction are presented in Table 2 and Figure 14.

Drilling depth (m)	Borehole diameter (inch)	Installation depth (m)	Casing length (m)	Casing diameter (inch)	Casing type
0.0–116.00	17 1/2"	0.00–112.70	112.70	13 3/8"	H–40
116.00–622.00	12 1/4"	0.00–618.70	618.70	9 5/8"	H–40
622.00–1744.50	8 1/2"	497.00–1744.00	1247.00	7"	H–40
1744.50–2202.2	6"	-	-	-	-

Table 4. Details of the Savica-1 well construction

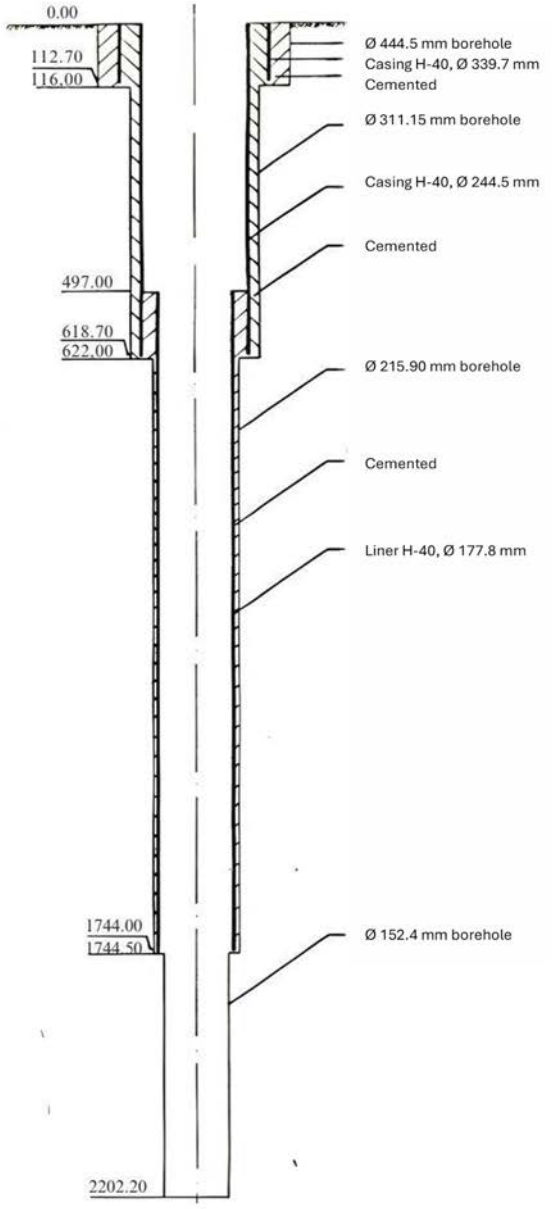

Figure 3.7. Well construction (Croatian Hydrocarbon Agency)

3.3.2. Geological-Geophysical Works and Special Operations at Savica-1

The development and testing of the well were carried out from June 30 to August 28, 1984. For the testing and cleaning of the well by swabbing, pipes of 2 7/8" (73.025 mm) diameter were installed down to a depth of 1740.58 m. Before the start of development, the amount of water flowing naturally was measured at 10 l/min (0.17 l/s). During the swabbing process, the quantity of water, temperature, and water level were measured. According to the data, for a swabbed water volume of 62 m³, the water level drawdown was approximately 140 m. The water temperature measured at the wellhead fluctuated between 22 and 52°C, while by the end of development the temperature stabilized and was recorded between 31 and 32°C.

A total of 5.7 meters was cored in two intervals:

1. Core (2013.8 – 2021.5 m):

The core was fragmented into several pieces, up to 2 cm in size. It consisted of white Lithothamnion limestone, breaking easily with an irregular fracture. Stratification was not pronounced. In addition to the dominant lithology, two small pieces of light brown platy limestone were present. These had a very light structure and broke easily.

2. Core (2021.5 – 2202.2 m): UV traces absent

The core was crushed, with fragments of heterogeneous composition. One fragment, approximately 10 cm long, was identified as breccia-conglomerate, composed of quartz, shale, and chert, with particle sizes ranging from 1 to 5 cm. The remaining fragments, up to 5 cm in size, consisted of quartz, shale, and dolomite, interpreted as pebbles derived from breccia-conglomerates. The matrix was clayey and reddish in color.

3.3.3. Conclusion of Drilling at Savica-1

The Savica–1 well partially fulfilled its intended objective. It penetrated the Lonja, Široko Polje, Kloštar–Ivanić, Ivanić Grad, and Prkos formations, and drilling was halted at a depth of 2202 m within the breccia-conglomerates of the Prečec Formation. The Tertiary basement rocks were found to lie deeper in this area than originally expected. The drilling rig Ideco II A could not continue the operation, which represented a significant setback, as previous drilling in this area had not captured the full stratigraphic sequence down to the Tertiary basement.

4. Geological Structure of the Geothermal Reservoir at the Potential Location and Broader Locations from Available Data

4.1. Geological Description

4.1.1. Lithology description for well Savica-1

The Savica-1 borehole penetrated deposits of the Lonja Formation, Široko Polje Formation, Kloštar Ivanić Formation, Ivanić Grad Formation, Prkos Formation and Prečec Formation (Table 5). Based on observations of sieve samples, calcimetry, coring tests, mud, and mechanical drilling speed, lithostratigraphic formations were determined, with the geological description of each formation provided in Table 6.

Formation	Interval (m)
Lonja Formation	0.0–882.0
Široko Polje Formation	882.0–1227.0
Kloštar Ivanić Formation	1227.0–1449.0
Ivanić Grad Formation	1449.0–1653.0
Prkos Formation	1653.0–1740.0
Prečec Formation	1740.0–2202.2

Table 5. Depth of Geological formations

Formation	Member	Interval (m)	Description
Lonja Formation		0.0–882.0	The formation is very heterogeneous. The upper part consists of alternating gravel, silty sand, and plastic clay. This is followed by gray-green marly clay and clayey marl, which alternate with layers of fine- to medium-grained sand and lignite.
Široko Polje Formation	Voloder Member	882.0–1039.0	Entirely composed of soft, highly clayey marl with interlayers of fine-grained, poorly consolidated sandstone.
	Krivaj Member	1039.0–1151.0	Identical in development to the previous member.
	Ježevo Member	1151.0–1227.0	Lithologically, it does not differ from the previous two members.
Kloštar Ivanić Formation		1227.0–1449.0	Composed of clayey marl with interlayers of fine, poorly consolidated sandstone.
Ivanić Grad Formation	Zagreb Member	1449.0–1521.0	This member is composed of clayey marl with interlayers of poorly cemented sandstone.
	Lipovec Marl	1521.0–1653.0	The upper part is built of clay and medium-hard marl, while the lower part is built of the silty, hard limestone-marl.
Prkos Formation		1653.0–1740.0	This formation is entirely composed of silty, hard, limestone-marl.
Prečec Formation		1740.0–2202.2	At a depth of 1740 m, Lithothamnion limestone was drilled, with a thickness of 95 m. Below the Lithothamnion limestone, dark grey, locally silty marl was encountered, and from 2000 – 2110 m,

	medium-grained quartz sandstone interlayers appear within the marl. At a depth of 2110 m, shale was drilled, and at 2130 m down to the bottom, a breccia-conglomerate composed of quartz pebbles, shale and chert.

Table 6. Geological description of the stratigraphic units on well Savica-1

4.2. Drill Stem Tests

Three Drill Stem Tests (DST) investigations were conducted on the Savica-1 well:

1. **DST**

The first DST test on the Savica-1 well was performed on August 16, 1981. in the interval 1717.0–1770 m, targeting the open hole section between 1744–1770 m. The test was carried out using an RTTS packer activated in the liner with a diameter of 177.8 mm (7") at a depth of 1717.0 m. The tested formation consisted of Lithothamnion limestones, from which an inflow of hot water was expected. The main objective of the test was to enable water flow to the surface, measure the yield capacity, and determine the temperature of the water both at the surface and within the borehole.

The test was entirely successful. The testing was fully successful. However, the upper manometer was fitted with an inadequate 12-hour chart mechanism (given the duration of the measurement), so the second static pressure was not recorded at all, and the second flow rate was recorded only partially. On the other hand, this manometer provided higher-quality records of the first flow rate and first static pressure curves compared to the diagram of the lower manometer, which enabled more reliable readings.

A total of 5.7 m^3 of water was obtained in the drill rods, calculated from the final pressure of second flow rate, this includes the volume of drilling fluid below the packer.

The water level in the drill rods was found at approximately 90 m from the surface. It was already evident from the pressure diagram that the tested interval had low permeability. This is supported by measurements: the pressure of first flow initially dropped to just 13.45 bar, while by the end of the second flow test it had increased to 162.69 bar.

As a result of the low permeability, extrapolated lines were obtained, whose slope appeared illogical. Specifically, the slope of the extrapolated line of the first static pressure (m_log = 45.3 bar) is steeper than that of the second static pressure (m_log = 5.04 bar). At first glance, it appears that there was formation damage due to drilling mud, which was removed during the second flow test, making the steeper extrapolated trend a result of improved permeability. However, the damage was not confirmed by calculations for either the first or the second measurement cycle, so this possibility is ruled out. The reason for the illogical pressure increase trend lies in the depression formed on the reservoir during the first flow measurement, resulting in partial energy loss. If the first flow period had lasted longer, the extrapolated line of the first static pressure would likely have been shallower, resulting in a higher m_log value.

During the second flow measurement, the rise of water column in drill rods acted as a barrier to the loss of formation energy. Given that it was measured over a long period, the reservoir was able to recover. As a result, the pressure increase during the second static pressure measurement was significantly faster. The extrapolated pressure line was much steeper, and *mlog* lower, which is characteristic of reservoirs with good to very good permeability (Kh).

If only a single measurement had been performed, such data would not have been obtained, since only the first static pressure would have been available for calculation. Likewise, if a water column of significantly greater height had been used, its pressure would not have allowed energy loss, and the pressure curves would have indicated more favorable permeability. The advantage of dual pressure measurement is more than evident in this case.

The first and second static pressure values *(mlog)* were used for the calculation, which resulted in significantly different final Kh values. This indicates the presence of zones with good to very good and low permeability around the borehole wall, with varying degrees of formation energy transmission. The dominant portion of the reservoir is of low permeability. The final extrapolated pressure is lower than the first one by 0.89 bar (≈ 0.90 atm). It is uncertain whether this is due to a pressure drop during the second flow test. This possibility is supported by the flow curves, which are mostly circular in shape, typically characteristic of reservoirs with limited lateral extent, or in this case, a permeable zone within a restricted area.

This represents an even less favorable characteristic of the tested section of the reservoir, given that it already shows inherently low permeability. Nevertheless, this interpretation should be treated with caution. The pressure of the formation water column at the measurement depth of 1714 m was 168.59 bar, which is 7.36 bar lower than the final extrapolated pressure (P_{extr} = 175.95 bar). This suggests that if the test duration had been long enough, the formation water would likely have flowed to the surface by itself.

The formation water sample, taken near the end of the reverse circulation phase and before the arrival of drilling mud. Due to its low salinity, it was likely diluted by surface water.

The daily yield, calculated from the flow rate curve, amounts to 54.84 m³ and this value was used for calculating other parameters. This represents the optimal inflow, which lasted only a few minutes and is used solely for estimating reservoir properties. It would be incorrect to assume that such a volume of water would continuously flow to the surface.

It should be noted that in the logbook for this and the following two tests, operators reported different volumes for the drilling rods Ø 88.9 mm per meter length: 3.85 l and 3.458 l, even though the same drill rods were used. Depending on which value is applied, different results are obtained, particularly the daily yield calculated from the flow curve. However, this does not significantly affect the overall interpretation of the tested interval.

The tested interval showed low permeability, with indications of a pressure drop in the reservoir layer due to limited collector permeability. Given the low overpressure, an “autonomous” inflow of the desired quantities of hot water could not have been expected. Temperature was not measured.

2. **DST**

The second DST test on the Savica-1 well was conducted on September 16 and 17, 1981, from the liner installed to a depth of 1744 m. The uncased section of the borehole channel between 1744 – 2202 m (length 458 m) was tested. The tested interval extended to a depth of 1847 m and consisted of Miocene Lithothamnion limestones, with deeper sections made up of variegated Oligocene conglomerates.

During this test, the packer was activated in the liner at a depth of 1708 m. A 514-meter water column was placed in the rods. At the beginning of the measurement, the inflow was low but soon became very intense. However, due to the rapid rise of the water level in the rods, a significant decline in air discharge was observed after about 10 minutes of testing.

During the test, the water level in the casing (drilling was performed with water) was unstable; instead of remaining steady, the well was constantly slightly overflowing. The measurement was continued with the

intention of repeating it if necessary. The first flow period lasted 61 minutes, and the static phase 89 minutes. No water reached the surface.

During the second flow period, after approximately 9 hours of measurement (04:25 h), the weak air discharge from the rods stopped, and a bit later (04:34 h) air suction was observed. It is assumed that the packer slipped, likely due to an increase in the weight of the tools caused by water entry. Half an hour later (05:03 h), the tools were lifted, and the load on the RTTS packer was reduced. Air release normalized, but the well continued to slightly overflow. After another half hour of testing, the packer was deactivated (05:15), assuming that it was no longer sealing at that depth, and that a shallower activation should be attempted. Re-activation was performed at 05:36 h at a depth of 1699 m. The water level in the well remained stable for a short time, but then the well began to overflow again. It was concluded that the packer was not sealing at this depth either, so the test was terminated by pulling the tools out at 07:25 h during the second flow phase.

No water reached the surface. After pulling the first stand of rods, the water level was below the surface, but with each subsequent removal, it returned to the same level; this was repetitive. It was obvious that water was leaking from the rods, but the location and cause were unclear.

The cause of the leakage could have been a defective circulation sub, drill rods, or testing tool. Water started to leak out when approximately 28 stands remained in the well, although no leakage point was detected on the rods.

According to the pressure diagrams, the measurement did not proceed normally. The first flow test was conducted normally, as was part of the second flow phase. During static pressure measurement, after 8 minutes a pressure drop was observed, followed by a further increase that was not characteristic of static pressure behavior. The pressure drop was likely caused by leakage in the testing tool.

During the second flow measurement, a more pronounced pressure drop occurred after 214 minutes, after which the pressure readings were generally stable. Because of these anomalies, the pressure diagrams were not suitable for reliable interpretation. Only the curve from the first flow period was considered usable, from which the daily yield was calculated to be 205.7 m^3. As the collected water sample was clearly identified as cushion water, the specific gravity applied in the calculations corresponded to that of the water from the first test (γ = 1.003 kg/dm^3). The temperature measured at a depth of 1708 m was 94.4 °C.

3. **DST**

The third DST test was conducted on September 17, 18, and 19, 1981, with the packer activated at a depth of 1686.22 m. During tool descent, no visible damage to the drill rods was observed. It was agreed in advance that a single measurement would be carried out, especially with the intention of recording the inflow for as long as possible. The inflow manifestation at the surface indicated very good production, similar to the previous test. However, the main difference was that the well level remained stable, showing only a slight downward trend.

Water reached the surface after 212 minutes of flow testing. The initial discharge rate was 4 liters per 3 minutes. The water temperature was 16.5 °C. After about 6 hours of testing, the discharge rate was 4 liters per 4 minutes. By the end of the second flow period, water was discharging at 0.5 liters per minute. The temperature was 15 °C, but it is not indicative, as it depended on the ambient air temperature; during the day it reached up to 22 °C due to solar heating.

During the test, in a conversation with on-site personnel, it was incidentally revealed that a metal object fell into the well several months earlier during tool lowering operations. This caused a blockage at 1551 m depth. During the instrumentation, it was noted that the tools unscrewed and fell to the bottom. This is

mentioned as a possible reason for potential casing damage, which may have led to communication behind the casing during the previous test. In such a case, pressure measurements would not yield reliable results.

To verify this assumption and check whether the drill rods were sealing properly, the dual was placed in the closed position and during the second static pressure measurement, the preventer was closed, and the annular space was pressurized to 50 atm. No pressure drop was observed during the 15-minute test. No unusual pressure increases were recorded on the diagrams. It was concluded that the test was successfully conducted.

From the readings of the lower pressure gauge, both the daily yield and the extrapolated static pressure were calculated. The daily yield is 339.60 m^3, which is significantly higher than that obtained from the previous test. The extrapolated static pressure amounts to 172.10 bars (175.49). Assuming the formation water has a specific weight of $\gamma = 1.003$, the hydrostatic pressure at a depth of 1684.14 m would be 6.45 bar (6.58 atm) lower than the extrapolated formation pressure. Since during flow testing, water with a salinity of up to 67 g/l and an average density of 1.0454 kg/dm^3 entered the rods, the hydrostatic pressure of this water column at the measurement depth would be 172.65 bar. This pressure exceeded the extrapolated formation pressure, indicating that the hydrostatic water column would have suppressed the reservoir and prevented natural flow to the surface.

Considering that the rods contained a 514 m column of fresh water, the fluid column described above managed to reach the surface. However, it is evident and supported by surface inflow measurements that, over time, the inflow of highly saline water would have suppressed the well.

To avoid confusion, it must be emphasized that this saline water does not represent formation water, but rather filtrate from drilling mud, with a salinity during drilling of up to 140 g/l. Given the high permeability, it is logical that filtrate losses occurred during drilling, possibly even damaging the reservoir. The lost filtrate was recovered during the test. These water samples are therefore not useful. When water appeared at the surface, there were 514 m of cushion water in the rods, with an assumed specific gravity of 1.0015 kg/dm^3, resulting in a hydrostatic pressure of 50.48 bar. The height of the saline water column, a filtrate with an average specific gravity of 1.0454 kg/dm^3, was 1166 m, corresponding to a pressure of 119.53 bar. From this, it followed that the fluid pressure in the rods at the moment of surface breakthrough was 170.02 bar. This calculated hydrostatic pressure corresponded to the pressure reading at 200 minutes of flow measurement, which was 169.46 bar

If the average pressure between 200 and 250 min of flow testing is used (i.e., 169.65 bar) and subtracted from the extrapolated static pressure of 172.10 bar, it follows that water began to discharge to the surface with an overpressure of 2.45 bar (2.498 atm). At the end of the flow test, the pressure reading was 171.08 bar, which is 1.02 bar lower than the extrapolated pressure, and thus represents the final discharge overpressure. Based on the salinity of water samples, it is evident that even after 32 hours and 55 minutes of testing, the cushion water was not replaced by formation water.

During the planning stage of testing, it was proposed to use nitrogen to accelerate the cleaning of the reservoir. By injecting it through flexible tubing, water would have been expelled from the rods during flow testing, thus accelerating inflow. Unfortunately, this was not implemented. The very steep curve of first Flow Period reflects high permeability, however, it should be noted that the open-hole section was also significantly long (458 m).

Calculations indicated significant damage within the tested interval. Given the high damage factor (DR = 5.12), the damage would have manifested even in extrapolated data, but the initial portion of the curve is obscured by tool vibrations during dual rotation. There is an interpretation that when testing highly permeable reservoirs, the effect of damage may appear even though it does not actually exist. Given the considerable loss of drilling fluid in this case, the possibility of damage cannot be ruled out a priori.

If damage occurred, the same parameters were recalculated excluding the damaged segment. The resulting values were significant. Calculations were carried out up to Kh, as the effective thickness is unknown. The temperature measured at a depth of 1687 m was 94.4 °C.

4.3. Characteristics of the Aquifer

Two chemical analyses of geothermal water are available for two different depth intervals: 1764–1769 m and 1699–2202 m. Two chemical analyses of water are available for two different depth intervals: 1764–1769 m and 1699–2202 m. The results of these analyses are presented in Tables 7 and 8. Additionally, water density, salinity, and pH were measured for the interval 1686.22–2202.00 m during the third DST test (Table 9).

Well	Savica-1
Date	17.08.1981.
Depth (m)	1764–1769
1. PHYSICAL CHARACTERISTICS	
1.1. Appearance	whitish, cloudy
1.2. pH	7.59
1.3. Density, 20°C, kg/dm³	1.003
1.4. Electrical resistivity, 20°C, Ω·m	2.72
2. CHEMICAL ANALYSIS	
2.1. Cations	mg/l
2.1.1. Ammonium (NH_4^+)	0.9
2.1.2. Sodium (Na^+)	924
2.1.3. Potassium (K^+)	34
2.1.4. Magnesium (Mg^{2+})	40
2.1.5. Calcium (Ca^{2+})	45
2.1.6. Strontium (Sr^{2+})	1.9
2.1.7. Iron (Fe^{2+})	-
2.1.8. Iron (total)	2.4
2.2. Anioni	mg/l
2.2.1. Chloride (Cl^-)	887
2.2.2. Bromide (Br^-)	0
2.2.3. Iodide (I^-)	0
2.2.4. Hydrogen carbonate (HCO_3^-)	1198
2.2.5. Carbonate (CO_3^{2-})	0
2.2.6. Sulfate (SO_4^{2-})	56
2.2.7. SiO2	49
Total dissolved salts	3186.9
Total dissolved salts (NaCl equivalent)	2312
Salinity	1.375

Table 7. Physical and chemical characteristics of geothermal water from the Savica-1 well (sampled at 1764–1769 m, 17 August 1981)

Well	Savica-1
Date	30.09.1981.
Depth (m)	1699–2202
1. PHYSICAL CHARACTERISTICS	
1.1. Appearance	clear
1.2. pH	7.92
1.3. Density, 20°C, kg/dm^3	-
1.4. Electrical resistivity, 20°C, Ω·m	8.47
2. CHEMICAL ANALYSIS	
2.1. Cations	mg/l
2.1.1. Ammonium (NH_4^+)	0
2.1.2. Sodium (Na^+)	143
2.1.3. Potassium (K^+)	2.35
2.1.4. Magnesium (Mg^{2+})	23
2.1.5. Calcium (Ca^{2+})	107
2.1.6. Strontium (Sr^{2+})	0.20
2.1.7. Iron (Fe^{2+})	-
2.1.8. Iron (total)	6.13
2.2. Anions	mg/l
2.2.1. Chloride (Cl^-)	243
2.2.2. Bromide (Br^-)	0
2.2.3. Iodide (I^-)	0
2.2.4. Hydrogen carbonate (HCO_3^-)	319
2.2.5. Carbonate (CO_3^{2-})	0
2.2.6. Sulfate (SO_4^{2-})	70
2.2.7. SiO2	0
Total dissolved salts	907.55
Total dissolved salts (NaCl equivalent)	-
Salinity	0.401

Table 8. Physical and chemical characteristics of geothermal water from the Savica-1 well (sampled at 1699–2202 m, 30 September 1981).

Sample		pH	Salinity (g NaCl/L)	ρ (20°C) (kg/dm³)
1.	SAVICA-1, DST-3 – interval 1686.22–2202 m, sampled on 19.09.1981	6.51	0.386	1.0013
2.	SAVICA-1, DST-3 – at the surface before closing, II section – from 6 pas	6.86	62.887	1.0451
3.	SAVICA-1, DST-3 – at the surface before closing, II section – from 2 pas	7.02	67.275	1.0453
4.	SAVICA-1, DST-3 – at the surface before closing, II section – from 6 pas	6.79	63.465	1.0454
5.	SAVICA-1, DST-3 – at the surface before closing, II section – from 6 pas	6.78	62.887	1.0455
6.	SAVICA-1, DST-3 – at the surface before closing, II section – from 10 pas	6.78	61.425	1.0455
7.	SAVICA-1, DST-3 – at the surface before closing, II section – from 12 pas	6.88	61.425	1.0453

Table 9. Results of water sampling from the Savica-1 well during DST-3

5. Geothermal Features of the Potential Location with Quantification of Possible Brine Production from the Current Well Assets and any New Drilling

5.1. Location

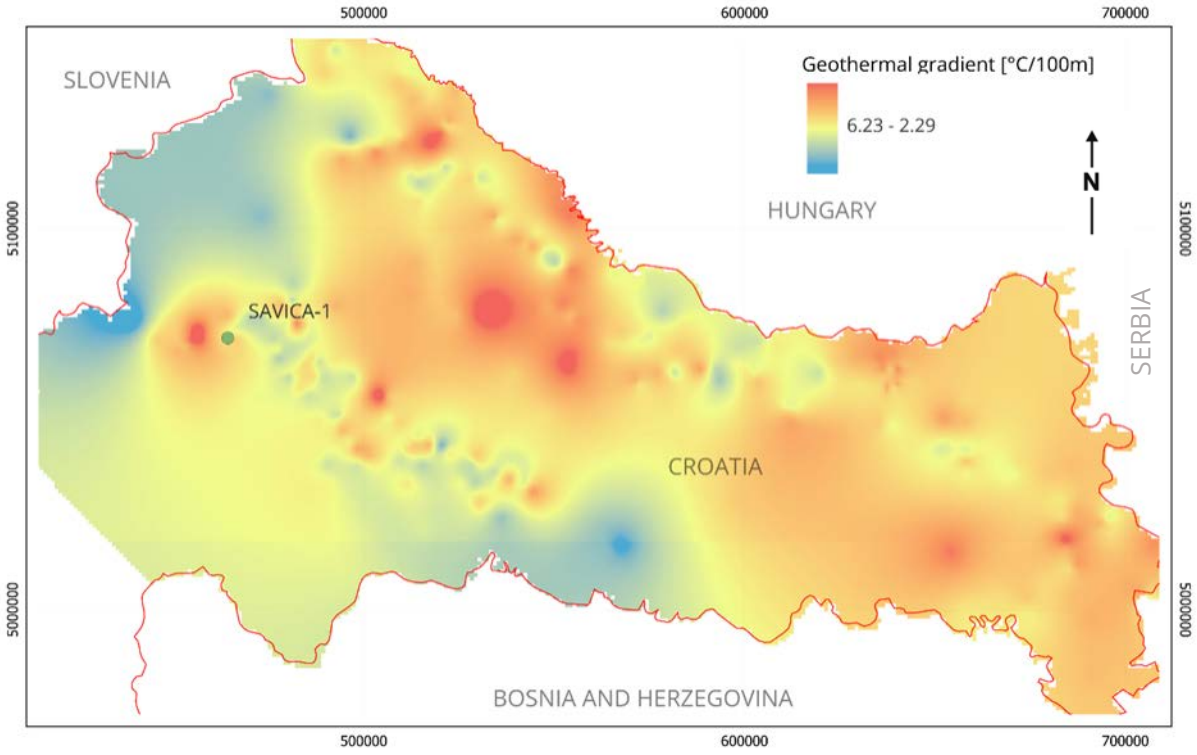

Figure 5.1. The geothermal map of Croatia (source: Croatian Hydrocarbon Agency)

For the assessment of geothermal energy potential, geothermal gradient and heat flow maps of the considered region are typically used. In the case of Croatia, this refers to the northern part of the country. The first to describe the thermogeological parameters of the Pannonian Basin was Jelić, who in his doctoral dissertation (1979) emphasized research of the Sava and Drava Depressions. The obtained relations characterized the thermogeological properties of both depressions. Based on these early investigations and published geothermal maps, it can be concluded that the Pannonian Basin in Croatia is suitable for geothermal energy utilization. This area is relatively well geologically explored, primarily due to extensive oil and gas exploration. More than 4,000 exploration, production, and development wells have been drilled, which, in addition to providing geological correlations and locating hydrocarbon reservoirs, also enabled the delineation of deep aquifers. Although a significant number of these wells have since been abandoned or decommissioned, the data collected during exploration still represent a valuable resource for evaluating the geothermal potential of the region. The geothermal map of Croatia (Figure 15) shows that the Savica site is characterized by a geothermal gradient of 3.8 °C/100 m, which is slightly above the global average of about 20–30 °C/km. In addition to the geothermal gradient, the assessment of local thermal properties provides a practical basis for optimizing the design and operation of BTES systems. For the Savica site, thermal rock properties were calculated using Jelić's correlations for thermal conductivity, heat capacity,

and density in the Sava basin, together with temperature data from the geological report for the Savica-1 well. In the following section, the correlations are described in more detail with reference to the Sava Depression, where the Savica-1 well is located.

5.2. Physical Properties of Rocks

For the estimation of physical rock parameters, values reported by Jelić (1979, 1984, 1987) were considered. His analysis included data from 147 wells in total (69 from the Sava Depression with 459 samples and 78 from the Drava Depression with 461 samples), from which correlations of average rock densities were established for both basins. In this study, correlations derived for the Sava Depression are applied, since the Savica-1 well is located within this geological setting.

Relationship between temperature and depth

Jelić (1979) noted that thermal conductivity can be estimated from correlations with other geophysical properties of rocks. In particular, he defined the relationship between thermal conductivity and density as:

$$k = 0.142 g^{2.86} \quad (5.1)$$

where:

k — thermal conductivity, W m^{-1} °C^{-1}

g — rock density, g cm^{-3}

In his analysis of density with depth, Jelić (1979) used density data from deep borehole cores and performed a statistical evaluation to establish systematic relationships between depth, density, and porosity. Based on this analysis, he expressed the density and average density of rocks in the Sava Depression as:

$$g_S = -0.792 e^{(-0.725d)} + 2.72 \quad (5.2)$$

$$g_{S,avg} = 1.092 \left(\frac{e^{(-0.725d)} - 1}{d} \right) + 2.72 \quad (5.3)$$

where:

g_S — average rock density in the Sava depressions at depth d, g cm^{-3}

e — base of the natural logarithm

d — depth, km

$g_{S,avg}$— mean average rock densities down to depth d in the Sava depression, g cm^{-3}

According to the same reference, the average ground surface temperature in the study area is:

$$T_0 = 11.6\ ^\circ\mathrm{C}$$

Based on the average heat flow and the relationship between geothermal gradients, heat flux, and conductivity, obtained from equations (5.1) and (5.3), the following equations describe the relationship between temperature and depth:

$$T_S = \frac{474 d^{3.86}}{[1.09(e^{-0.72d} - 1) + 2.72d]^{2.86}} + 11.6 \quad (5.4)$$

where:

T_S — average temperatures at depth d, °C

d — depth, km

e — base of the natural logarithm

Equations (5.4) represent complex function, which can be approximated using standard mathematical procedures with simpler parabolic functions. The resulting functions deviate by ±4% from the original values and are expressed as:

$$T_S = 50.37d^{0.779} + 11.6 \quad (5.5)$$

where:

T_S — average temperatures in the Sava depression at depth d, °C

d — depth, km

The mean average temperatures down to a given depth are obtained by integrating equation (5.5) and dividing by depth:

$$T_{S,avg} = 28.31d^{0.779} + 11.6 \quad (5.6)$$

where:

$T_{S,avg}$ — mean average temperatures down to depth d in the Sava depression, °C

d — depth, km

Relationship between specific heat capacity of rocks and depth

The specific heat capacity of rocks depends on the specific heat of the rock matrix, porosity, and the specific heat of the pore-filling fluid. According to the literature, the specific heat capacity of the rock matrix of most rocks is about 0.7 J $g^{-1}K^{-1}$. This value varies with temperature, and according to G. Buntebarth (1980), it can be expressed as:

$$c_m = 0.75(1 + 6.14 \times 10^{-4}T - 1.982 \times 10^{-7}T^{-2}) \quad (5.7)$$

where:

c_m— specific heat capacity of the rock matrix, J $g^{-1}K^{-1}$

T — temperature, K

Rock temperatures were calculated using equation (5.6) and inserted into equation (5.7). Thus, the specific heat capacity of the rock matrix with depth in the Sava depression was obtained.

For the pore-filling fluid, water was assumed. The specific heat capacity of water increases with rising temperature but decreases with rising pressure. It was also assumed that water pressure increases hydrostatically with depth, and that temperature rises according to equation (5.4).

From the average densities, the average porosities were also determined, as well as the systematic relationship of these properties with depth. Based on porosity data obtained from well log measurements in sandstones of various formations within the Sava Depression, Jelić (1984) expressed the average porosity–depth relationship as:

$$\varphi_S = 46e^{-0.725d} \quad (5.8)$$

where:

φ_S — average rock porosity in the Sava depression at depth d, %

e — base of the natural logarithm

d — depth, km

The specific heat capacity of rocks, considering porosity, the specific heat of the matrix and water, average water density of 1 g cm^{-3}, and average matrix density of 2.72 g cm^{-3}, can be calculated as:

$$c = \varphi \times c_v \times \frac{1}{g} + (1 - \emptyset) c_m \frac{2.72}{g} \quad (5.9)$$

where:

c — specific heat capacity of rocks, J g^{-1}K^{-1}

φ — porosity (fractional value)

c_v — specific heat of water, J g^{-1}K^{-1}

c_m— specific heat of the rock matrix, J g^{-1}K^{-1}

g — rock density, g cm^{-3}

Based on the above considerations of matrix and water heat capacities, density, and porosity, the specific heat capacity of rocks in the Sava depression was calculated with depth.

The decrease in rock specific heat capacity with depth is consistent with the decrease in porosity, as this is a consequence of the relatively higher specific heat of water compared to the matrix. Thus, the rock specific heat capacity decreases with depth due to the reduction in water content (Jelić, 1987).

The specific heat capacity of rocks decreases with depth due to the reduction in water content. For the relationship between depth and rock specific heat, a simple exponential function was assumed. This function was determined using a standard fitting method, as follows:

$$c_S = 0.602e^{-1.177d} + 0.898 \quad (5.10)$$

where:

c_S — specific heat capacity of rocks in the Sava depression at depth d, J g^{-1}K^{-1}

e — base of the natural logarithm

d — depth, km

The mean values of specific heat capacity down to a given depth can be obtained by integrating equations (5.10) and dividing by depth:

$$c_{Savg} = -\frac{0.511}{d}\left(e^{-1.177d} - 1\right) + 0.898 \quad (5.11)$$

where:

c_{Savg} — mean specific heat capacity of rocks down to depth d in the Sava and depression, J g^{-1}K^{-1}

e — base of the natural logarithm

The calculated depth profiles of thermal conductivity, volumetric heat capacity, and temperature for the Savica site are shown in Figure 16.

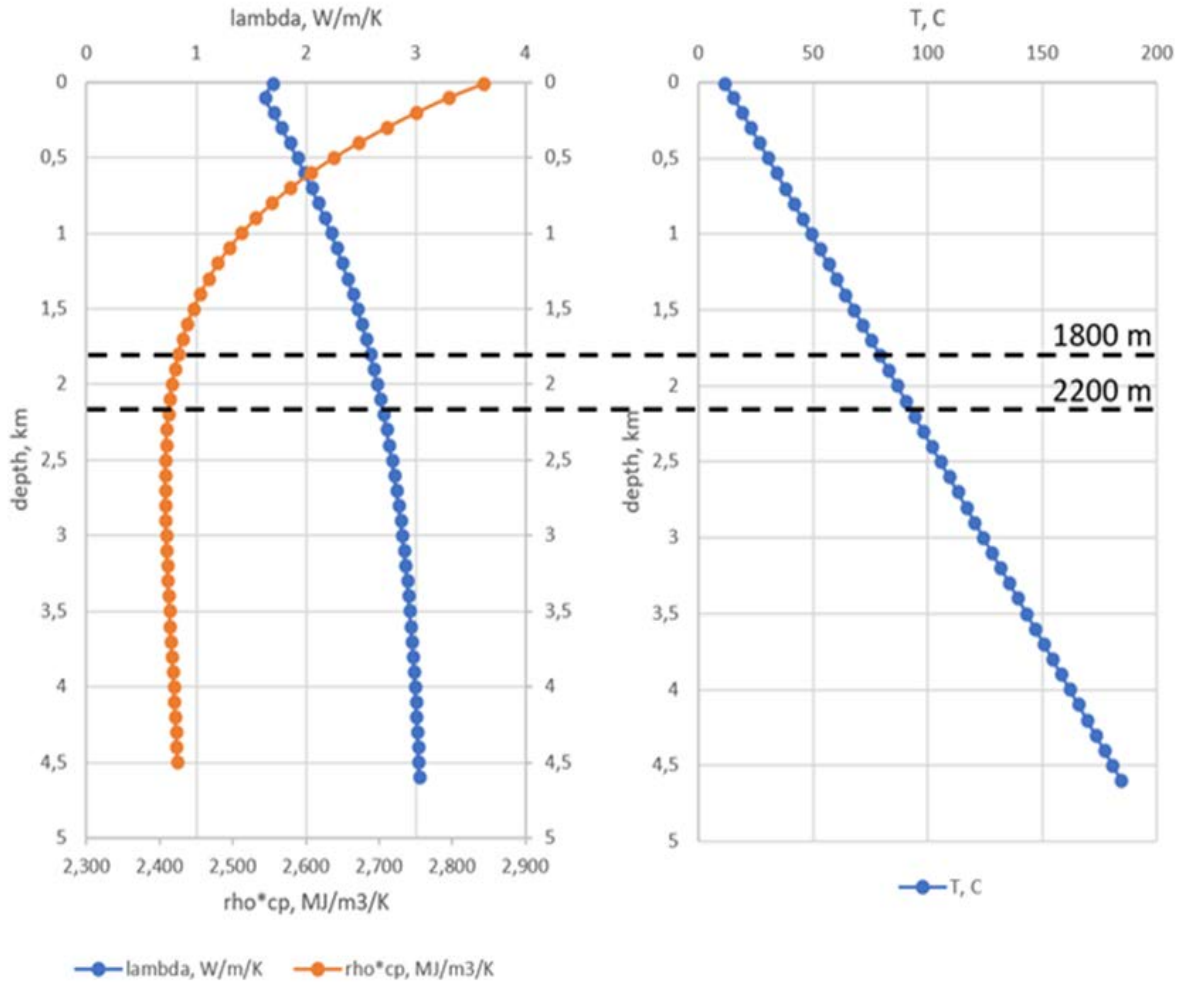

Figure 5.2. Thermophysical rock properties at Savica-1 well based on Jelić correlations for Sava subbasin (Jelić, 1987) and geological report for Savica-1 well.

6. Extraction and Definition of the Geothermal Potential of the Area with Defining the Technical-Technological Aspects of Energy Use of Geothermal Brine for Electricity Production with ORC Technology and/or Direct Use in District Heating

As described in subsection 4.2 Drill Stem Tests, the measured flow rates were 0.63 l/s (DST 1), 2.38 l/s (DST 2), and 3.93 l/s (DST 3). Because of its low brine production capacity and its location in the city's industrial zone close to a cogeneration power plant, the Savica-1 well was chosen as a pilot site for borehole thermal energy storage (BTES). To assess the feasibility of repurposing the well, a numerical modelling framework was developed.

The modelling framework is based on transient simulation of energy balance flows in the surface equipment, borehole heat exchanger (BHE) and the geothermal reservoir. The simulation is done in a coupled approach for all three system components modelled by separate balance equations. The modelling framework for the BHE is built on 1D energy balance for coaxial BHE with annular inlet (CXA exchanger – coaxial annular inlet). The modelling framework for the geothermal reservoir is finite element analysis (FEM). Both BHE and reservoir modelling approach are done in a commercially available software FeFlow (Diersch, 2014). For finite element groundwater flow in FeFlow, relevant data and case studies can be found in (Diersch, 2014) or in the FeFlow online documentation (FeFlow 8.0 Documentation). Surface equipment is modelled with user-defined scripts in which all model features are combined with a set of specific equations describing each of the component. The full coupling is done with a Python-Feflow interface. The framework is tested on a hypothetical case study for a single-well BHE (acting as a single-well deep BTES) integrated into a district heating (DH) network of the city of Zagreb. The location of the BHE corresponds to the existing Savica-1 well located in the industrial zone of the city of Zagreb, but also in a relative proximity to the potential heat demand. The conceptual scheme of the problem is presented in Figure 17. As a transition towards the 4th generation district heating (Lund et al., 2021) and decarbonized heating, the BTES is introduced. During the winter period, the DH is supplied directly from the BHE and industrial waste heat, where BHE is used first. During the summer period industry is rejecting the excess heat due to limited flexibility. In combination with this waste heat and lack of thermal demand, the BHE could now be used to reject the heat into the reservoir to enhance its thermal recovery before the new heating season starts. Since in this work only a single deep BHE is considered, it can balance heat flows for only one minor part of the DH, i.e. DH covering residential object in the proximity of the BHE and source of industrial waste heat. Therefore, the DH network is divided into DH-1 and DH-2, where only DH-1 has the direct access to the BHE as a part of the BTES in seasonal balancing between industrial waste heat and heat demand. The waste heat thermal power is few tenths to few hundreds of megawatts, while a single BHE can be used to accept up to a few hundreds of kilowatts, depending on the configuration. From the modelling point of view, the effects of a single well would not be visible in the modelling results if the division between DH-1 and DH-2 was not done. In this report, all further modelling and analysis of results will refer only to DH-1, where the effect of single BHE of the BTES can be visible. The detailed scheme of the process is presented in Figure 18. As already mentioned, only the DH-1 (the one containing the BHE) is relevant for the analysis. The system consists of three heat exchangers (HX): the main heat exchanger for direct heating with geothermal energy (HX) and two waste heat exchangers (WH 1 and WH-2) for utilization of industrial waste heat. The WH-1 is used to additionally heat the DH-1 during the heating season if the geothermal reservoir fails to supply

sufficient heat in terms of both DH-1 and leaving load temperature (LLT). The WH-2 is used to reheat the geothermal reservoir during the summer time when there is excess heat from the industry and no heat demand. A high temperature heat pump (HTHP) is used to elevate the temperature level of the low-enthalpy geothermal heat. As a final heating supply for the DH-1 there is a possibility to use the electric heating (EH). Electric heater should be used only if there is not enough heat supply from the WH, heat pump or direct use of geothermal heat from HX.

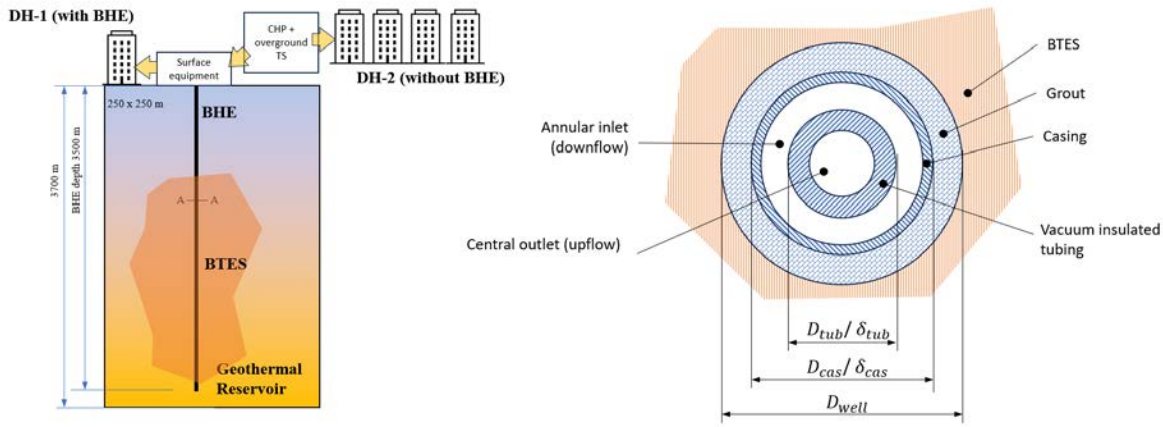

Figure 6.1. The conceptual scheme of the simulation problem (left) and cross-section of the borehole heat exchanger with annular inlet BHE-CXA (right)

All three HX's can be bypassed with the use of three separate two-way valves V-HX, V-WH1 and V-WH2, which are used to control the mass flow at the „hot" side of the HX and consequent heat transfers in heat exchangers.

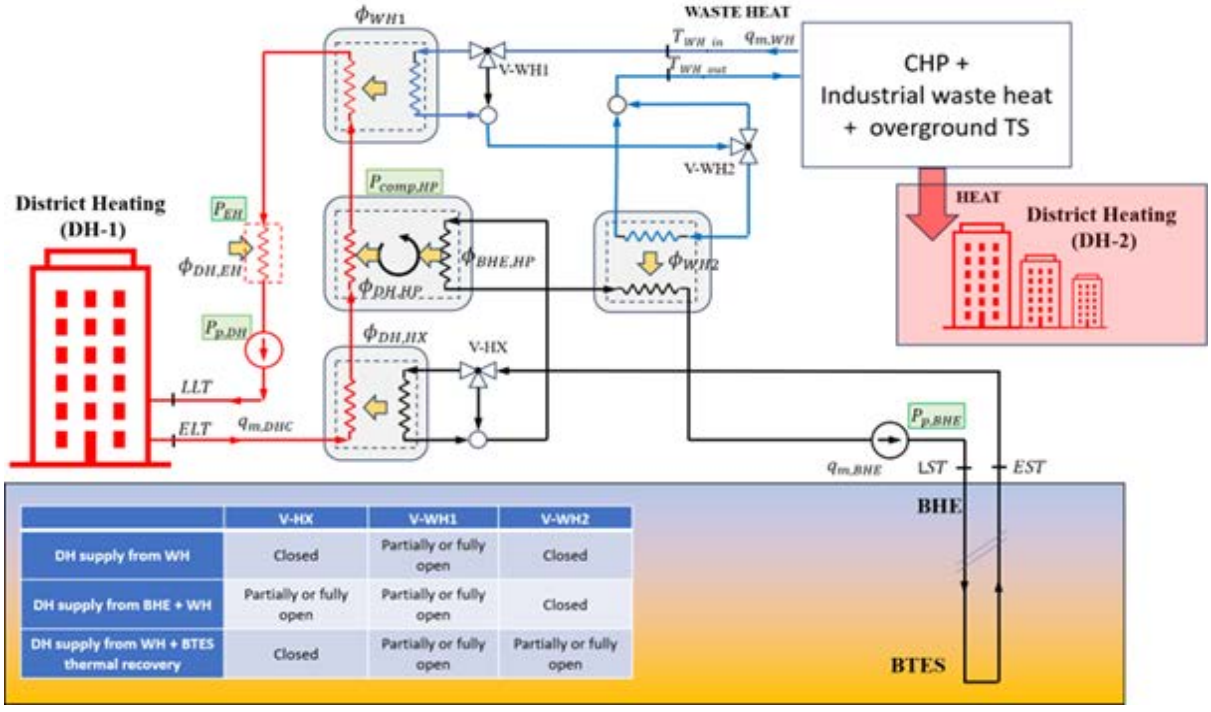

	V-HX	V-WH1	V-WH2
DH supply from WH	Closed	Partially or fully open	Closed
DH supply from BHE + WH	Partially or fully open	Partially or fully open	Closed
DH supply from WH + BTES thermal recovery	Closed	Partially or fully open	Partially or fully open

Figure 6.2. The scheme of surface equipment with energy flows of heat and electricity

The mass flow rate on the „hot“ side of the HX is determined by the valve openness ratio x_v (Equation 6.1).

$$x_v = \frac{q_{m,HX}}{q_m} \tag{6.1}$$

which is a ratio between the mass flow rate going through the heat exchanger $q_{(m, HX)}$ and total mass flow rate q_m (Equation 6.2).

$$q_m = x_v q_{m\_q_{m,HX}} + (1 - x_v) q_{m\_q_{m,HX,bypass}} \tag{6.2}$$

The value of valve openness ratio x_v lies between 0 and 1.

The role of surface equipment is to ensure the best possible way to:

- extract geothermal heat for direct heating of DH-1 from BHE-CXA and WH-1 during the heating season
- store excess heat from the WH-2 into the geothermal reservoir through the BHE-CXA into the reservoir

The overall energy balance consists from the heat and power balance. Heat balance has to satisfy temperature constraints, meaning that inlet temperature from waste heat is $T_{wh,in}$ and is determined by the operation of the industrial burners. The leaving source and entering source temperatures, LST and EST, are determined by the operating strategy of the surface equipment and is described in detail in the following chapters. The leaving load and entering load temperatures, LLT and ELT, are determined by the heat demand of the system, which can be high-temperature or low-temperature, depending on the heating system DH-1.

Future DH systems will eventually evolve into the low-temperature systems with temperatures in the system lower than 60 °C, but the full transition will take a few decades.

The overall modelling framework is presented in Figure 19.

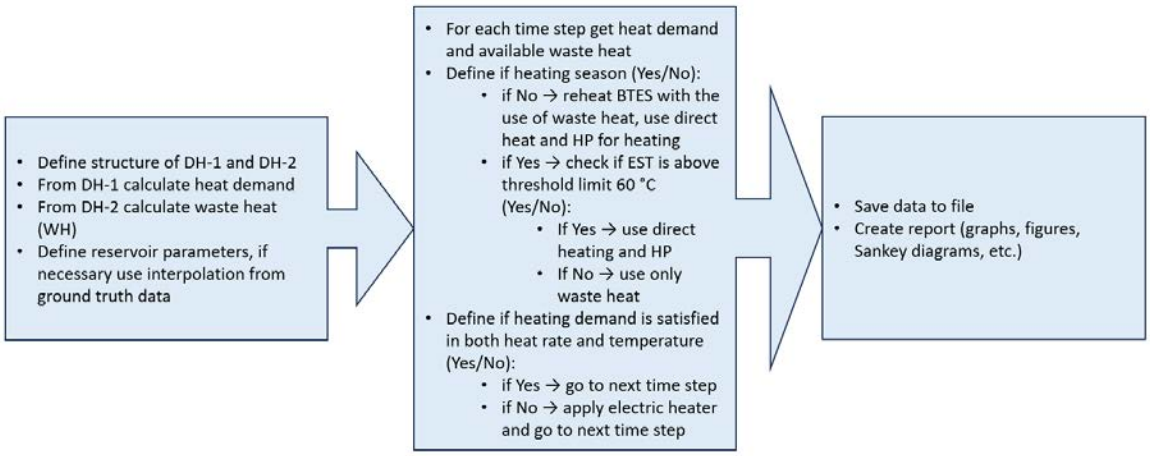

Figure 6.3. The overall modelling framework of the BTES assessment method

The modelling is done with transient simulation, since seasonal variations in energy flows have to be captured. The control of the surface equipment combining waste heat and BHE is done with control valves V-HX, V-WH1 and V-WH2. The coupling between the surface operation and reservoir modelling is done with the use of a Python-Feflow interface.

The detailed description of the mathematical modelling of heat exchangers, together with optimization of the valve openness x_v is given below.

- The Python-FeFlow interface

The Python v3.10 (Pilgrim & Willison, 2009) interface is written in Spyder Python IDE, and dynamic update of FeFlow BHE boundary conditions is done with the use of FeFlow's Interface Manager (IFM) (IFM FEFLOW Model Class). The interface is based on a time-stepping algorithm that takes into account pre-time step and post-time step processes that govern the operating parameters of the BHE-CXA prior to FEM calculation.

In the pre-time step the mass flow rate ($q_{m,BHE}$) and leaving source temperature (LST) are calculated from the balance of the overall surface equipment. In the post-time step the resulting entering source temperature (EST) is obtained from the FEM calculations in the current time step and all results for the current time step are saved into the result file. The complete interface is presented in Figure 20.

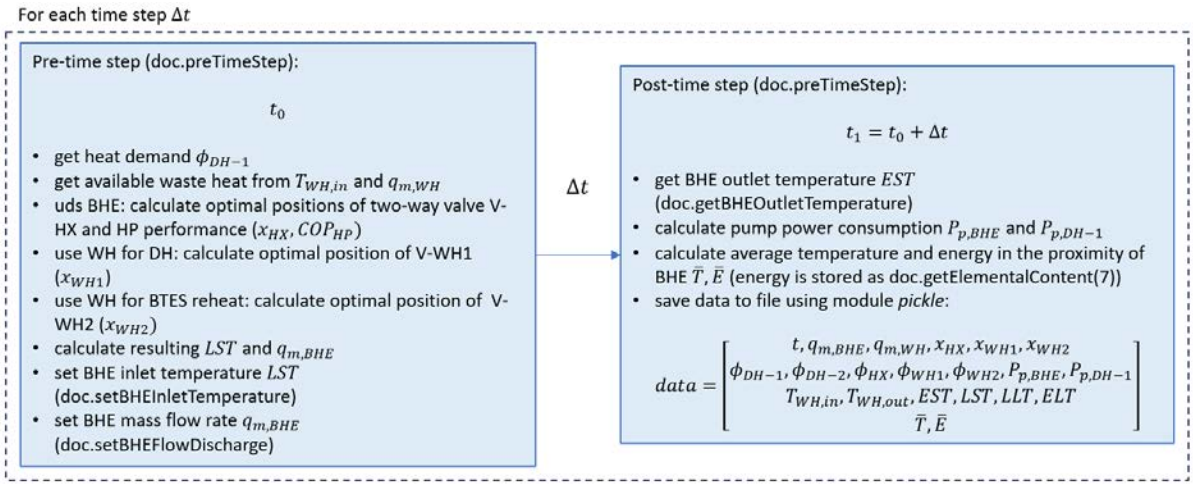

Figure 6.4. The Python-Feflow interface

Available waste heat is provided as available inlet temperature ($T_{WH,in}$) at given mass flow rate ($q_{m,WH}$). The coupling between the surface equipment and the FeFlow is done with optimization of mass flow rates which control heat transfer in each of the heat exchanger. Mass flow rates are directly dependent on the openness of control valves ($x_{v,HX}, x_{v,WH1}, x_{v,WH2}$). The detailed description and mathematical model of heat demand and heat exchanger is provided in following chapters.

- The DH-1 heat and power demand

The heat demand is calculated from the formula (Equation 6.3):

$$\phi_{DH-1} = q_{m,DH-1} c (LLT - ELT) \tag{6.3}$$

where LLT is determined by the ambient temperature and heat to be delivered ϕ_{DH-1} is determined by the mass flow rate of the DH-1 system $q_{m,DH-1}$. The parameter c is specific heat of the water.

Power demand is determined by the consumption of circulation pumps which are function of mass flow rate, density and pressure drop in the system. There are two circulation pumps, one for primary fluid that ensures

the flow rate between the BHE and surface equipment $P_{p,BHE}$, and other one for DH-1 mass flow rate between surface equipment and heating demand $P_{p,DH-1}$. The power consumption is calculated according to the Equation (6.4):

$$P_p = \frac{q_m}{\rho} \Delta p \tag{6.4}$$

Pressure drop Δp is calculated from the Bernoulli equation, where pressure drop dominantly depends on linear pressure drop that is calculated from the Equation 6.5:

$$\Delta p_{lin} = \frac{fL}{D} \frac{1}{2} \frac{1}{\rho} \left(\frac{q_m}{A}\right)^2 \tag{6.5}$$

The friction factor *f* is calculated iteratively from the Colebrook-White relation.

- Water-to-water heat exchanger (WTW-HX)

The water-to-water (WTW) heat exchangers (HX) are modelled based on NTU method. The role of the WTW HX model is to find outlet hot (H) and cold (C) stream temperatures according to Figure 5. Implicit statement of the problem can be written as (Equation 6.6):

$$F\left(q_{m,H}, T_{H,in}, T_{H,out}, q_{m,C}, T_{C,in}, T_{C,out}, \phi\right) = 0 \tag{6.6}$$

Variables $\left(q_{m,H}, T_{H,in}, T_{H,out}, q_{m,C}, T_{C,in}, T_{C,out}, \phi\right)$ are operating parameters and (c_C, c_H, k, A) are physical parameters and constants. Depending on the unknowns to be found, the explicit formulation can be derived. For example, if the inlet temperatures of the cold $T_{C,in}$ and hot $T_{H,in}$, stream as well as cold stream mass flow rate $q_{m,C}$ and heat demand ϕ are known, then the problem becomes (Equation 6.7):

$$\left(q_{m,H}, T_{H,out}, T_{C,out}\right) = f\left(T_{H,in}, q_{m,C}, T_{C,in}, \phi\right) \tag{6.7}$$

Usually there are practical limits to of outlet temperatures $T_{H,out}$ and $T_{C,out}$ and in that case the heat transfer rate ϕ cannot be known in advance, but becomes a solution of a constrained nonlinear optimization problem where the outlet temperature of the cold stream is now a part of the goal function. The scheme of the problem is presented in Figure 21.

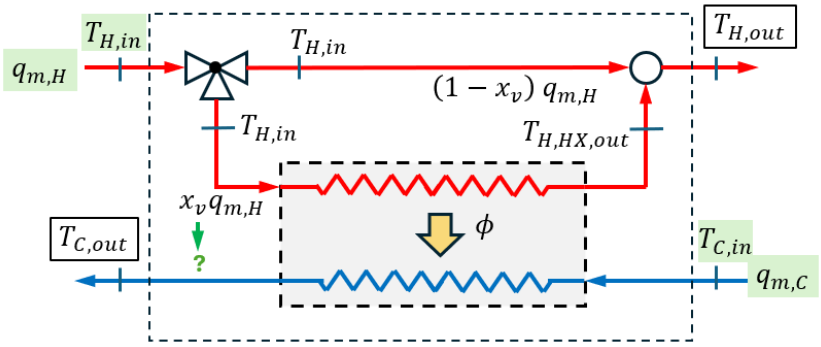

Figure 6.5. Scheme of the optimization problem

The problem statement referring to Figure 6-5 is: find the position of a two-way valve x_v which will ensure that $T_{C,out}$ is as close as possible to predefined value $T_{C,out,set}$ without violating the minimum outlet temperature of the hot stream $T_{H,out,min}$ or maximum outlet temperature of the cold stream $T_{C,out,max}$. The goal function is (Equation 6.8):

$$min\left(\left|T_{C,out} - T_{C,out,set}\right|\right) = f(x_v) \qquad (6.8)$$
$$0 \le x_v \le 1$$

subject to constraints (Equation 6.9):

$$T_{H,out} > T_{H,out,min} \qquad (6.9)$$
$$T_{C,out,max} > T_{C,out}$$

Variables $\left(T_{C,out,set}, T_{H,out,min}, T_{C,out,max}, q_{m,H}, T_{H,in}, q_{m,C}, T_{C,in}\right)$ should be know in advance. The goal function brings $T_{C,out}$ as close as possible to $T_{C,out,set}$ by changing the bounded variable x_v which should be low enough to avoid $T_{H,out}$ below the minimum value of $T_{H,out,min}$ or $T_{C,out}$ above the minimum value of $T_{C,out,max}$, but high enough to minimize the goal function.

The goal function is calculated from the following expression (Equation 6.10):

$$min\left(\left|T_{C,out} - T_{C,out,set}\right|\right) \qquad (6.10)$$

where $T_{C,out}$ and resulting ϕ can be calculated from the following set of equations for ϕ and x_v (Equation 6.11):

$$T_{C,out} - T_{C,in} - \frac{\phi}{C_C} = 0 \qquad (6.11)$$

$$\left\{\frac{1-e^{\left[-\frac{kA}{C_{min}}\left(1-\frac{min\left(C_C,x_v q_{m,H} c_H\right)}{max\left(C_C,x_v q_{m,H} c_H\right)}\right)\right]}}{1-\frac{min\left(C_C,x_v q_{m,H} c_H\right)}{max\left(C_C,x_v q_{m,H} c_H\right)}e^{\left[-\frac{kA}{C_{min}}\left(1-\frac{min\left(C_C,x_v q_{m,H} c_H\right)}{max\left(C_C,x_v q_{m,H} c_H\right)}\right)\right]}}\right\} \times min\left(C_C,x_v q_{m,H} c_H\right)\left(T_{H,in}-T_{C,in}\right)-\phi=0$$

If the temperature at the exit of the HX on the side of the hot stream is noted as $T_{H,HX,out}$, then the resulting temperature at the hot side can be calculated from the mixing balance (Equation 6.12 and 6.13):

$$T_{H,out}=x_v T_{H,HX,out}+(1-x_v)T_{H,in} \tag{6.12}$$

with

$$T_{H,HX,out}=T_{H,in}-\frac{\phi}{x_v q_{m,H} c_H} \tag{6.13}$$

The constraints can be calculated from the expressions (Equation 6.14):

$$\begin{gathered} T_{C,out,max}-T_{C,in}-\frac{\phi}{C_C}\geq 0 \\ x_v\left(T_{H,in}-\frac{\phi}{x_v q_{m,H} c_H}\right)+(1-x_v)T_{H,in}-T_{H,out,min}\geq 0 \end{gathered} \tag{6.14}$$

The mass flow rate through the hot side of the HX is (Equation 6.15):

$$q_{m,H,HX}=x_v q_{m,H} \tag{6.15}$$

The x_v represents the openess ratio of the valve and is calculated as (Equation 6.16):

$$x_v=\frac{q_{m,H,HX}}{q_{m,H}} \tag{6.16}$$

- High temperature heat pump model (HTHP)

District heating heat pumps for 4th generation district heating systems must increase the temperature level of heat from temperatures of 10-15 °C up to 60-65 °C. This represents the high-temperature heat pump (HTHP) category. In this work the detailed modelling of HTHP will not be presented, since it is out of the scope, but simple model based on temperature difference is presented in Figure 22.

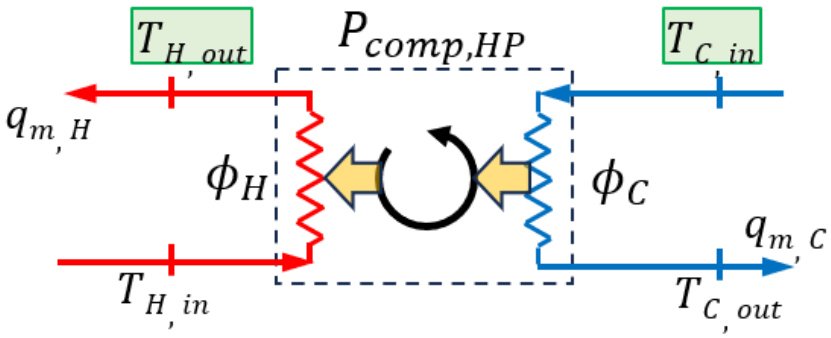

Figure 6.6. Scheme of the heat pump as a reference to simple HP model

The model is based on coefficient of performance (COP), which can be defined, according to Figure 6-6, as (Equation 6.17):

$$COP_{HP} = \frac{\phi_H}{P_{comp}} = f(\Delta T_{HP}) \tag{6.17}$$

The heat pump temperature lift, ΔT_{HP}, can be calculated as difference between outlet of hot stream minus inlet of cold stream (Equation 6.18):

$$\Delta T_{HP} = T_{H,out} - T_{C,in} \tag{6.18}$$

The aim of the HTHP model is to maximize the heating rate ϕ_H with finding the optimal temperatures $T_{C,out}$ and $T_{H,out}$ which satisfy temperature constraints (Equation 6.19):

$$\begin{gathered} (\phi_H) \\ \phi_H = q_{m,H} c_w (T_{H,out} - T_{H,in}) \\ P_{comp,HP} = \frac{\phi_H}{COP_{HP}} \\ \phi_C = \phi_H - P_{comp,HP} \\ T_{C,out} = T_{C,in} - \frac{\phi_C}{q_{m,C} c_w} \end{gathered} \tag{6.19}$$

These temperature constraints are (Equation 6.20):

$$\begin{gathered} T_{H,out} \leq T_{H,out,max} \\ T_{C,out} \geq T_{C,out,min} \end{gathered} \tag{6.20}$$

The temperatures $T_{H,in}$ and $T_{C,in}$, as well as mass flow rates $q_{m,H}$ and $q_{m,C}$ need to be known in advance. An overview of HTHP's with corresponding functions $COP = f(\Delta T_{HP})$ is provided in Royo et al. (2021).

- Model of the borehole thermal energy storage (BTES) energy balance

In order to evaluate the possibility of a reservoir to store thermal energy, energy balance has to be done. Energy balance is based on energy conservation law (Equation 6.21):

$$\left(\frac{dE_R}{dt}\right)|_{r\leq r_{set}} = \phi_R|_{r=r_{set}} - \phi_{BHE} \tag{6.21}$$

Where the temporal term $\frac{dE_R}{dt}$ and the heat exchange with the BHE ϕ_{BHE} can be obtained from FeFlow simulations for the domain around then BHE satisfying the spatial condition $r \leq r_{set}$. If the temporal term is positive, heat is accumulated, and vice versa. The recovery heat power of the reservoir can be calculated (Equation 6.22):

$$\phi_R|_{r=r_{set}} = \left(\frac{dE_R}{dt}\right)|_{r\leq r_{set}} + \phi_{BHE} \tag{6.22}$$

This parameter is important since it reflects the inflow or outflow of heat from the proximity of the BHE. It depends on temperature regime in the BHE, as well as thermal and hydraulic properties of the reservoir and groundwater movement. It reflects both conductive and convective term, and if the convective term is known, the conduction term can be calculated.

6.1. Determination of Working Conditions

- Setup of Savica-1 in FeFlow

In this work two BHE configurations for Savica-1 well will be tested. According to insulated tubes that can be placed in a well casing, the two possibilities are tested: one that is inserted in a shallower, but wider well and can be placed up to 1800 m depth and another that is inserted in deeper, but narrower well and can be placed up to 2200 m depth. The main parameters of these two BHE options are listed in Table 10.

Parameter	Unit	Values		Description
		BHE2200	BHE1800	
L_{well}	m	2200	1800	well depth
D_{well}	in	6.00	8.50	well diameter
	mm	152.40	215.90	
$D_{cas,OD}$	in	5.50	7.00	tubing OD
	mm	139.70	177.80	
δ_{cas}	in	0.24	0.50	tubing thickness
	mm	6.20	12.65	
$D_{cas,ID}$	in	5.01	6.00	tubing ID
	mm	127.30	152.50	
$D_{tub,OD}$	in	3.50	4.50	vacuum tube OD
	mm	88.90	114.30	

$D_{tub,ID}$	mm	50.60	76.00	vacuum tube ID
δ_{tub}	mm	19.15	19.15	vacuum tube thickness
A_{ann}	mm2	6518	8001	annulus area
A_{cen}	mm2	2010	4534	central tube area
w_{ann}	m/s	0.77	0.62	annulus area fluid velocity based on 5 kg/s
w_{cen}	m/s	2.49	1.10	central area fluid velocity based on 5 kg/s

Table 10. Borehole heat exchanger parameters for 1800 and 2200 m depth

Moreover, BTES will be compared to cases with no BTES reheating. Reheating is done from the second waste heat HX (see Figure 6-2). So, for no-reheat the valve V-WH2 is fully closed at all times. The complete list of all cases is presented in Table 11.

Case name	Deep borehole heat exchanger	Waste heat source	BTES reheating
BHE1800-Ind-RehY	BHE1800	Industrial	Yes
BHE2200-Ind-RehY	BHE2200	Industrial	Yes
BHE1800-Ind-RehN	BHE1800	Industrial	No
BHE2200-Ind-RehN	BHE2200	Industrial	No

Table 11. Setup of Savica-1 well test cases

The thermal conductivity of the casing is taken as 50 W/m/K, for the grout 2.3 W/m/K and for the vacuum insulated tubing 0.015 W/m/K (class D grade of insulation). Thermal rock properties were calculated using Jelić correlations for thermal conductivity, heat capacity and density for Sava subbasin (Jelić, 1987) and temperature from the geological report for Savica-1 to determine geothermal gradient and graphically presented in Figure 23.

The boundary conditions of the Feflow domain are no-flow isothermal, where boundary temperature corresponds to the static temperature. The assumption is that reservoir is isothermal at the boundaries, with bottom temperature equal to 160 °C, temperature at the top equal to 12 °C and lateral boundaries at linear distribution between the top and the bottom (Figure 12). This results in thermal gradient of approx. 40 °C/km. The mesh is triangular in x-y plane and resolution is approximately 0.5 meters around the BHE and 10 m on the lateral boundary. Depth is set to 2500 m and layers are equidistant in z-direction. The domain is modelled as a dry rock, with porosity of 5% and zero hydraulic conductivity.

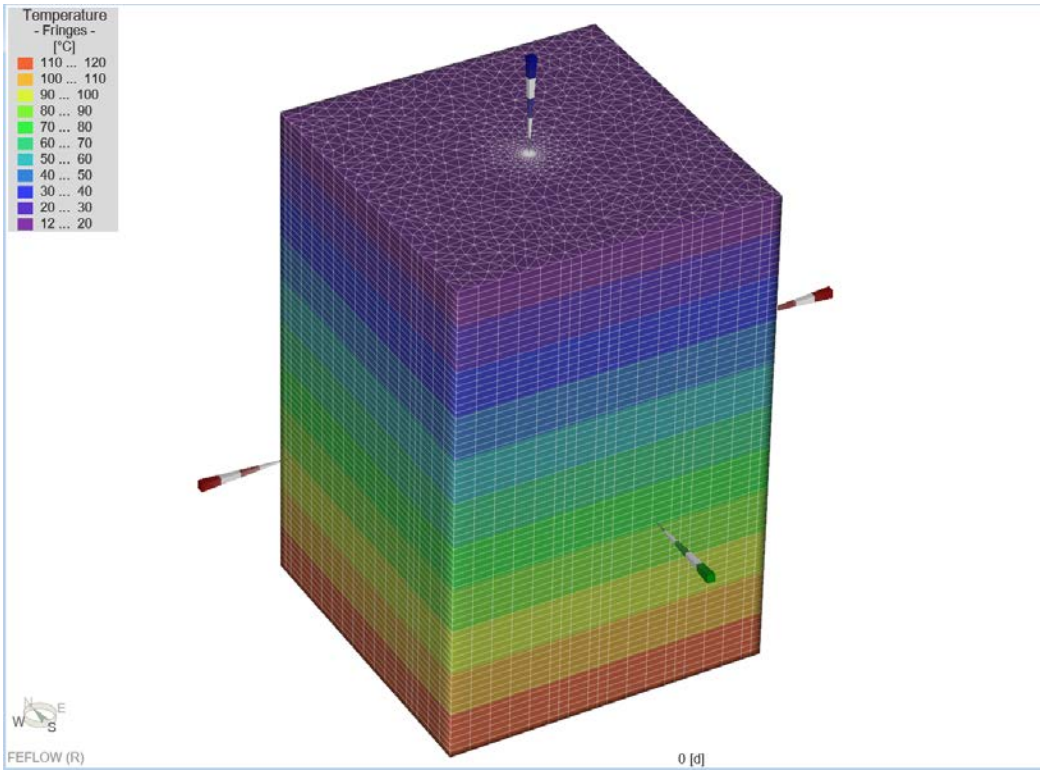

Figure 6.7. FeFlow domain around Savica-1 well with isothermal boundary conditions

- Setup of parameters in Python interface for modelling industrial waste heat and heat demand

The total heat demand of DH-1 is calculated as 2 GWh. The hourly distribution of thermal demand is calculated as (Equation 6.23):

$$\phi_{DH,t} = \delta_t \phi_{dem,tot} \tag{6.23}$$

where δ_t is a fraction of heat demand in time „t“ calculated as (Equation 6.24):

$$\delta_t = \frac{d_t}{\sum_{t=1}^{8760} d_t} \tag{6.24}$$

and $d_t = 0.627 - 0.0258 \times T_{amb,t}$. Therefore, hourly distribution of heat demand depends on hourly distribution of ambient temperature $T_{amb,t}$.

The LLT of the DH-1 depends also linearly on the ambient temperature (Equation 6.25):

$$LLT = 80 + \frac{65 - 80}{20 - 5}\left(T_{amb,t} - 5\right) \tag{6.25}$$

The values are cropped between $65 \leq LLT \leq 80$. The sliding parameter is mass flow rate of the waste heat hot water (Equation 6.26):

$$q_{m,WH,t} = \frac{\phi_{DH,t}}{(LLT - ELT)4200} \quad (6.26)$$

Industrial waste heat is modelled with a constant temperature of 80 °C. The timeseries of input setup variables for DH-1 for a single year are presented in Figure 24.

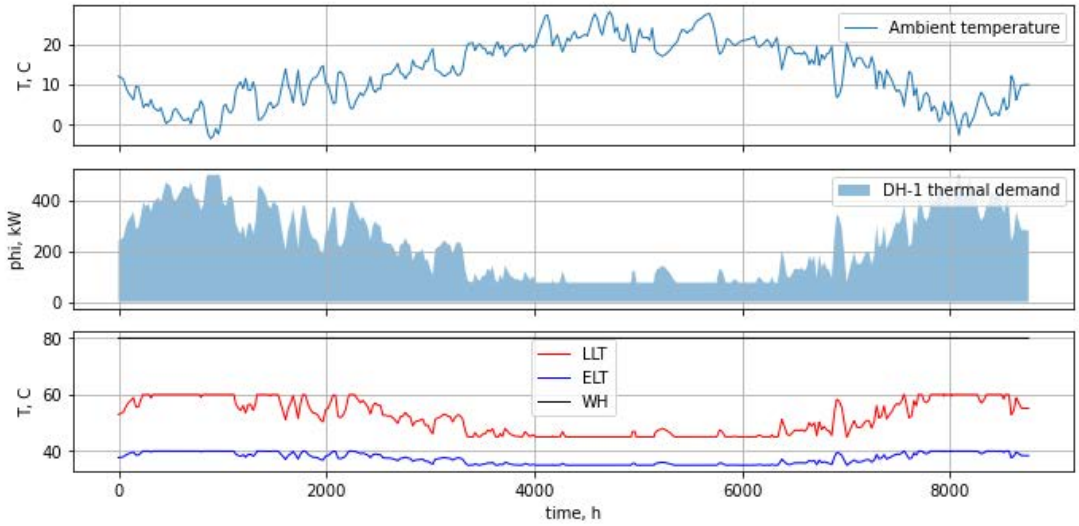

Figure 6.8. Annual timeseries of input variables

The peak thermal demand is around 500 kW during the winter season for heating and hot water demand and less than 100 kW during the summer season for hot water demand. For a multi-Year analysis the annual timeseries of input data are repeated.

Analysis of results: annual energy balance for all cases

Annual energy results are presented in Figure 25 for the second Year of simulation. Results differ substantially between configurations and whether reservoir reheating was included into the system. Power balance (a) shows big difference between power consumption between BHE1800 and BHE2200 configurations, which was expected due to hydraulic losses for longer BHE with smaller tubing diameter for case BHE2200. However, power consumption for electric heater was larger for BHE1800, while power consumption of HTHP compressor was larger for BHE2200. Power consumption shows little difference between reheating and no reheating. DH balance (b) shows that DH supply is dominated by HTHP in all cases, while direct heat supply from the BHE is negligible for cases with no reheating. Second largest heat supplier is from the waste heat WH-1, while electric heating generally has minor influence on heat supply. The total annual heat demand equals to the predefined value of 2GWh. BHE balance (c) shows that the reservoir is the main supplier of heat towards the BHE, while for the reheating cases substantial role has also the waste heat at WH-2. Withdrawal of heat from the BHE is dominantly for HTHP, while for reheating there is also a smaller portion of direct heating. WH balance (d) shows that reheating mainly influences the WH-2, and lowest WH supply is for the case of BHE2200 with no reheating.

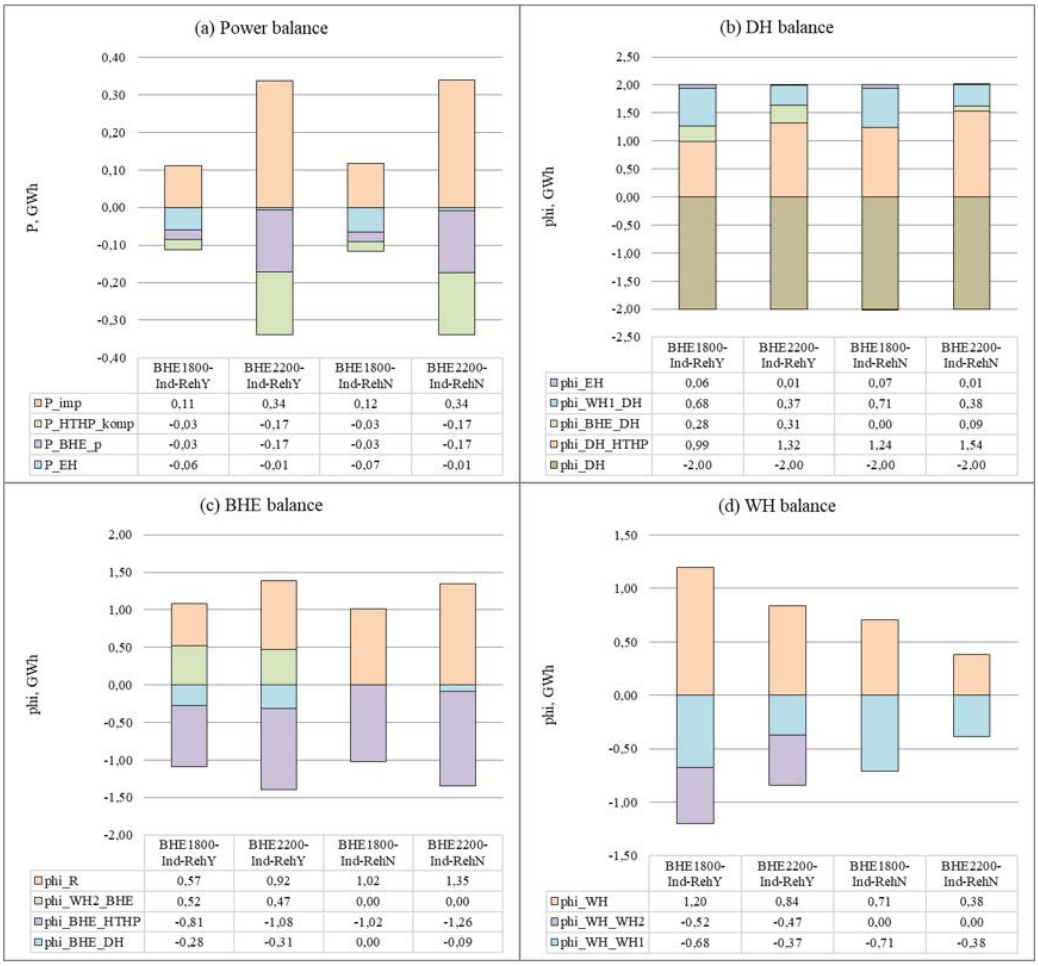

	BHE1800-Ind-RehY	BHE2200-Ind-RehY	BHE1800-Ind-RehN	BHE2200-Ind-RehN
P_imp	0,11	0,34	0,12	0,34
P_HTHP_komp	-0,03	-0,17	-0,03	-0,17
P_BHE_p	-0,03	-0,17	-0,03	-0,17
P_EH	-0,06	-0,01	-0,07	-0,01

	BHE1800-Ind-RehY	BHE2200-Ind-RehY	BHE1800-Ind-RehN	BHE2200-Ind-RehN
phi_EH	0,06	0,01	0,07	0,01
phi_WH1_DH	0,68	0,37	0,71	0,38
phi_BHE_DH	0,28	0,31	0,00	0,09
phi_DH_HTHP	0,99	1,32	1,24	1,54
phi_DH	-2,00	-2,00	-2,00	-2,00

	BHE1800-Ind-RehY	BHE2200-Ind-RehY	BHE1800-Ind-RehN	BHE2200-Ind-RehN
phi_R	0,57	0,92	1,02	1,35
phi_WH2_BHE	0,52	0,47	0,00	0,00
phi_BHE_HTHP	-0,81	-1,08	-1,02	-1,26
phi_BHE_DH	-0,28	-0,31	0,00	-0,09

	BHE1800-Ind-RehY	BHE2200-Ind-RehY	BHE1800-Ind-RehN	BHE2200-Ind-RehN
phi_WH	1,20	0,84	0,71	0,38
phi_WH_WH2	-0,52	-0,47	0,00	0,00
phi_WH_WH1	-0,68	-0,37	-0,71	-0,38

Figure 6.9. Annual energy results for all cases

1. Analysis of results: estimation of BTES performance and system efficiencies

In order to see the dynamics of BTES, the timeseries of BTES energy is presented in Figure 6-10. The energy is estimated from the formula (24) as integral of derivation of reservoir energy within certain radius from the BHE. Reservoir energy is obtained from the FeFlow internal IFM functions.

$$E_{BTES} = \int_{t=0}^{8760h} \left(\frac{dE_R}{dt}\right)|_{r \le r_{set}} \qquad (30)$$

In this work a radius of r_{set} = 4 m around the BHE is considered as a BTES volume. Results show that without reheating BTES can regenerate naturally from the surrounding geothermal heat. Without reheating energy recovery starts at – 100 MWh and ends at + 100 MWh for BHE1800 and +180 for BHE2200 meaning that natural regeneration can add approximately 200 and 280 MWh, respectively. If reheating (WH-2) is included, then additional 250 MWh for BHE1800 and 220 MWh for BHE2200 can be added to BTES. For a 400 kW demand this corresponds to approx. 625 and 550 additional hours of heating, respectively.

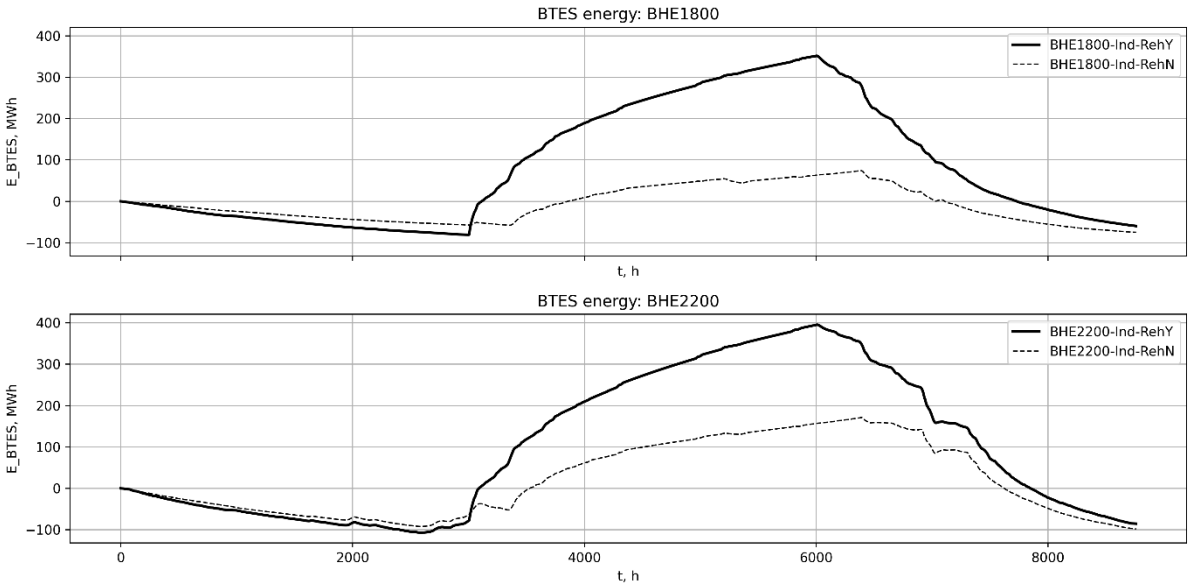

Figure 6-10. Timeseries of BTES energy

The efficiency comparison will be done according to the parameters COP_{HTHP} and COP_{tot}. They are defined according to the equations

$$COP_{HTHP} = \frac{\phi_{DH,HTHP}}{P_{HTHP,komp}} \tag{31}$$

$$COP_{tot} = \frac{\phi_{DH}}{P_{HTHP,komp} + P_{BHE,pump} + P_{EH}} \tag{32}$$

which define internal HTHP efficiency and overall efficiency of the heating system. Efficiency results are presented in Figure 26.

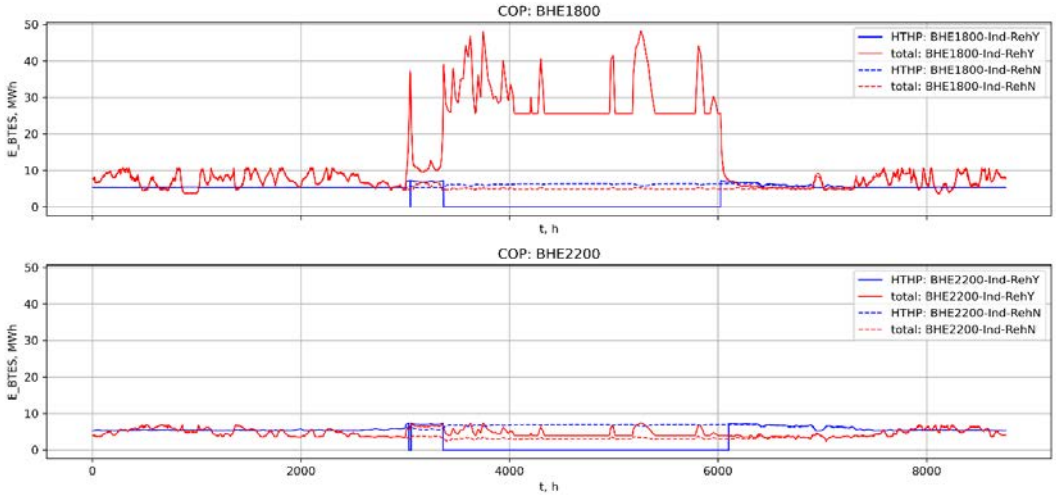

Figure 6.10. Comparison between system efficiencies for all cases

For the BHE1800 values of total COP are slightly higher than for the BHE 2200. On the other hand, HTHP COP is around 7 for all cases, since it depends only on temperature difference, as described in the method chapter.

2. Analysis of results: detailed timeseries results for the case BHE1800-Ind-RehY

To illustrate the dynamics of the energy flows, the detailed timeseries for the second Year of simulation is presented in Figure 27.

Analysis shows that direct heating from BHE is dominant when heat demand is low. This is during the summer for covering the hot water demand. Direct heating will be applied only when EST is above 5 °C difference from the LLT. Valve openness (*x*) also shows that reheating WH-2 is active during the summer period, while for winter heating season WH-1 covers the heat demand above baseload BHE supply. Electric heaters are supplying only peak thermal demand.

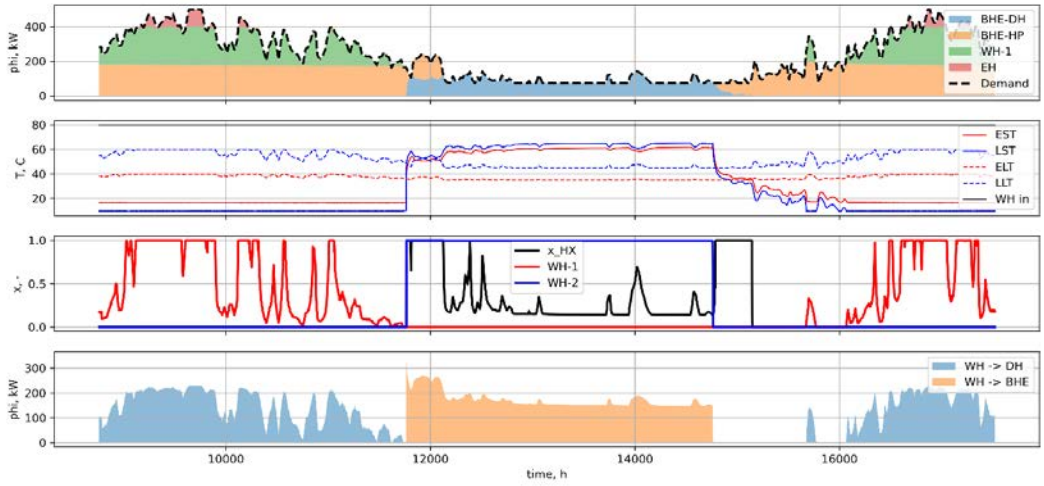

Figure 6.11. Detailed timeseries analysis for the second simulation year for the 1800 m deep BHE with reheating (case BHE1800-Ind-RehY).

Requirements to reuse hydrocarbon wells for Borehole Thermal Energy Storage

A total of four configurations have been tested with difference in length and diameter of the casing and whether reheating is included or not. All four tested cases showed different annual energy flows, indicating the need for a-priori testing presented in this report.

Main conclusions are that longer tubing leads to higher hydraulic losses and higher power consumption, but reduces the need for the waste heat, which is favourable if waste heat comes at high cost. Also, longer tubing can reach higher temperatures at greater depths and can provide higher amount of direct heating. The influence of using reheating as BTES leads to the the higher heat supply from the waste heat for reheating and higher supply of direct heating from the geothermal for supplying the district heating when compared to no-reheating cases.

When considering the amount of energy that was recovered in BTES, case with shorter BHE can recover more heat than the case with longer BHE, since temperatures at bigger depths are comparable with waste heat temperatures which reduces the heat transfer. However, future work should analyse the use of geothermal reservoir at lower depths to reduce hydraulic losses on the expense of reduced DBHE exchange area.

7. Environmental Features of the Project from the Perspective of Environmental Impact

7.1. Analysis of Environmental Features of the Project from the Perspective of Environmental Impact

7.1.1. Impact on Biodiversity

Although mining-related activities are planned during the execution of the project, no significant impact on protected natural areas is expected, as the Savica-1 well is located outside of ecological network zones in accordance with the applicable spatial planning documentation. The location of the Savica-1 well lies within an industrial zone (Žitnjak), which has already been anthropogenically altered, and no protected natural habitats or designated Natura 2000 areas are directly affected.

Nevertheless, it is necessary to analyze the presence of endangered or rare habitat types in the broader and narrower project area, especially in the immediate surroundings of the well pad and along potential utility or pipeline corridors in case of future redevelopment. Since the wellhead area occupies a relatively small surface and considering that the construction and testing activities are time-limited, significant negative impacts on local flora and fauna are not expected.

Temporary impacts on biodiversity may occur during potential refurbishment works, primarily due to vegetation removal, noise, vibrations, and the presence of machinery and personnel. These impacts will be short-term and spatially limited. If additional installations are developed at the Savica-1 site, any permanent changes to soil and habitat structure will be minimized and confined to already altered zones within the industrial area.

Under regular operating conditions, the exploitation of geothermal water at the Savica-1 well should not have a negative impact on biodiversity in the narrower or wider area. More intense impacts on flora and fauna are possible only in the case of accidental situations involving the uncontrolled release of geothermal water or spillage of fuels or working fluids

7.1.2. Impact on Geodiversity

In order to determine the impact on geodiversity in the Žitnjak area, where the Savica-1 well is located, it is necessary to analyze the presence of geodiversity in terms of geological and geomorphological diversity that could be disrupted. In addition, the potential presence of geological and paleontological natural monuments within or near the area will be assessed. Based on currently available data, it can be preliminarily concluded that the project, during regular operations, will not have a negative impact on the geodiversity of the area.

7.1.3. Impact on Water

The potential future use of geothermal water from the Savica-1 well will be conducted through a closed-loop system, where water is transported from the production well to the injection well through sealed pipelines. The well is fully cased, cemented, and hermetically sealed, preventing the possibility of geothermal water infiltrating potable aquifers.

During regular operation, no additives or chemicals will be used in any of the technological processes. The system is designed to prevent contact of geothermal water with the environment and oxygen, which could

affect mineralization and equipment corrosion. After heat extraction, the cooled geothermal water will be reinjected into the reservoir.

Therefore, the exploitation of geothermal water at the Savica-1 site is not expected to have a negative impact on surface or groundwater, including drinking water sources protected by sanitary zones.

Potential negative impacts, depending on the type of incident, may occur in the event of accidental leakage of geothermal water or spillage of working fluids or fuels during refurbishment or transport operations. These impacts will generally be spatially limited and short-term due to timely response and application of remediation measures.

7.1.4. Impact on Soil

The construction and use of the Savica-1 well may have a negligible impact on the soil, primarily due to temporary or permanent repurposing of land within the well platform and access roads. Under normal operating conditions, the technological system will not cause adverse effects on soil. Temporary disturbances may occur during preparatory or refurbishment work, and in case of accidental spillage of geothermal water or other fluids. Due to the salinity of geothermal water, larger spills may lead to short-term soil contamination. These impacts are expected to be spatially limited and reversible, provided remediation measures are implemented promptly.

7.1.5. Impact on Air Quality

The impact on air and microclimate at the Savica-1 site is expected to be minimal. There will be no significant losses of thermal energy to the environment. No emissions of harmful or odorous gases are expected during regular operation, and no negative impact on nearby residential areas is foreseen. Laboratory analyses of geothermal water indicate only minor presence of dissolved gases (primarily CO_2 and traces of methane), so in the event of an accidental release, the impact on air quality would be negligible and short-term.

7.1.6. Impact on Landscape

The impact of the geothermal water exploitation at the Savica-1 site on the landscape will be minimal. The wellhead occupies a small area and is located within an existing industrial zone (Žitnjak), where it does not represent a visual or spatial disturbance. In case of future installation of additional above-ground infrastructure (e.g. separator or heat exchanger), appropriate landscaping and visual integration measures will be implemented to minimize its visibility and ensure it blends into the existing urban-industrial surroundings.

7.1.7. Impact on Cultural Heritage

Due to the location of the Savica-1 well within an industrial area and at a considerable distance from protected cultural monuments, historical structures, or archaeological sites, no impact on cultural-historical heritage is expected. The nature of the project and its spatial scope do not pose a threat to cultural values.

7.1.8. Noise Impact

During regular operation, the exploitation of geothermal water at the Savica-1 well will not generate noise levels above permissible limits. Circulation and injection pumps, if installed, will operate with low noise levels and will not disturb the surrounding area. Occasional noise may occur due to personal vehicle movement or maintenance activities, but this will remain within acceptable environmental standards. Potential short-term increases in noise are expected during future refurbishment or drilling operations, which will be spatially limited and temporary.

7.1.9. Waste Generation

During regular operation of the Savica-1 well, no waste is expected to be generated. Waste produced during construction, refurbishment, or testing works (e.g. lubricants, drilling fluids, and municipal waste from staff presence) will be collected and disposed of through authorized legal entities. Hazardous waste, such as used oils or chemical residues, will be handled in accordance with valid regulations and contractual arrangements with licensed waste management companies. In the event of an accidental situation (e.g. fluid spill, equipment failure), timely remediation will ensure that any environmental impact is spatially limited and short-term.

7.1.10. Environmental Accidents and Risk of Their Occurrence

In the event of an environmental accident (e.g. uncontrolled release of geothermal water), technical measures will be implemented to stop the release and minimize environmental impact. Due to the salinity of geothermal water, accidental discharge of larger volumes may temporarily contaminate the soil, but the closed nature of the system significantly reduces the likelihood of such an event. No flammable or explosive substances will be used during regular operation. Given the low level of risk and the controlled technological setup, the probability of accidents is considered minimal.

7.1.11. Environmental Impacts After Exploitation Cessation

After the exploitation of the Savica-1 well is concluded, no long-term environmental impacts are expected. Upon project completion, above-ground installations will be removed, and the well will be technically decommissioned in accordance with professional standards. The land will be rehabilitated and returned to its original state or adapted to the intended land use in agreement with local stakeholders

7.1.12. Cross-border Environmental Impacts

Given the project's location within the urban area of Zagreb and its distance from national borders, no transboundary or global environmental impacts are expected as a result of the Savica-1 geothermal well project.

7.1.13. Environmental Protection Measures

Based on its location, scope, and technical design, the environmental impact of the Savica-1 project is expected to be negligible under normal operating conditions. The main environmental protection measure is the application of a closed-loop system for the circulation, use, and reinjection of geothermal water. Additionally, all technological systems and equipment will be operated under professional supervision, and work procedures will follow prescribed occupational health and environmental safety protocols.

These measures apply across all project phases, including potential preparatory works, operation, refurbishment, and response to accidental events.

7.1.14. Activity Monitoring

If required by competent authorities (e.g., Hrvatske vode), monitoring wells (piezometers) may be installed for the observation of groundwater quality in nearby aquifers. Regular inspections and maintenance of the system will ensure continued compliance with environmental protection regulations and operational safety standards.

7.2. Conclusion of Environmental Features of the Project

The exploitation of geothermal water from the Savica-1 well is spatially limited to the area where the geothermal aquifer has been identified, meaning that the environmental impact of its potential future use

will be of local significance. The environmental impact of using geothermal water for heating purposes, or of constructing potential supporting installations at the Savica-1 site, primarily depends on the geological-structural and hydrogeological characteristics of the reservoir, the physico-chemical properties of the geothermal fluid, and the technical-technological characteristics of the system.

Potential environmental impacts may be associated with the presence of gases dissolved in the geothermal water, particularly carbon dioxide in carbonate reservoirs and methane or other hydrocarbon gases in sandstone or gas-adjacent reservoirs. In addition to these, nitrogen, hydrogen sulfide (H_2S), mercury, and radon may also occur in smaller concentrations, depending on site-specific reservoir conditions.

Should geothermal exploitation at the Savica-1 site be activated, any gases released at wellhead pressure will need to be captured and reinjected into the reservoir together with the geothermal water. This approach extends the operational lifespan of the reservoir, reduces greenhouse gas emissions, and maintains pressure balance in the geothermal system, particularly if elevated concentrations of dissolved gases are present.

If technically and economically feasible, the separated gas could be used as an additional energy source (e.g., via microturbines for internal consumption or for reheating secondary fluid circuits). However, in all cases, carbon dioxide as a combustion product must be captured and reinjected into the reservoir to prevent its release into the atmosphere.

With proper application of these reinjection practices, the system for geothermal exploitation at Savica-1, if reactivated, could operate as an environmentally responsible, low-emission system with no significant atmospheric impact under normal operating conditions.

8. Analysis of the Feasibility of Investing in a Geothermal Field at the Potential Location with the Aim of Producing Electrical and Thermal Energy

8.1. Introduction for economic analysis once investment starts

An analysis of investments in mining facilities for geothermal energy exploitation considers the final price of both thermal and electrical energy (for OPEX) to estimate potential revenue under the framework of the Renewable Energy Sources and High-Efficiency Cogeneration Act (OG 138/2021, 83/2023), the Regulation on the Promotion of Electricity Generation from Renewable Energy Sources and High-Efficiency Cogeneration (OG 70/2023), the Regulation on Quotas for Promotion of Electricity Generation from Renewable Energy Sources and High-Efficiency Cogeneration (OG 57/20), and the State Aid Program for Market-Premium Support for Electricity Generation from Renewables and High-Efficiency Cogeneration 2021–2023, published by HROTE. For the revenue calculation, different heat energy prices must be considered. One reference is the heat energy price applied by HEP for industrial consumers, which amounts to approximately 45.4 EUR/MWh. Considering the comparison with natural gas prices, it is necessary to account for both the price level and its future trends, which are currently very difficult to predict. In Croatia, domestic natural gas production has been continuously decreasing, and in 2023 only 15.1% of total gas consumption was covered by domestic production. Despite new fields planned for development and new production wells expected to increase domestic output, more than 80% of demand will need to be met by imported gas in the coming period. In this way, the Croatian natural gas market is directly linked to price movements at European gas

hubs, primarily the Central European Gas Hub (CEGH). Geopolitical factors have had a drastic impact on the European energy market in recent years, and the current situation can be described as a recovery from the energy crisis. Maintaining lower prices of gas and oil, and consequently electricity, in the coming period will directly depend on political developments, in particular the continuation of the war between the Russian Federation and Ukraine, as well as economic sanctions imposed by the European Union in response, and on geopolitical events in other parts of the world, especially the Middle East. Although current prices are lower compared to the extreme highs recently recorded for electricity, gas, and oil, this only further highlights the economic and strategic importance of investing in renewable energy sources and strengthening energy supply security.

The technological option under consideration is the repurposing of the existing Savica-1 well as a deep BHE for borehole thermal energy storage. The concept relies on a single retrofitted well, located in the industrial zone of Zagreb and in proximity to potential heat demand, which could be integrated into the local district heating (DH) network. To exploit the thermal energy storage potential of the proposed Savica-1 well and when considering the technological option that includes revitalization of the well, mining works listed in Table 12are required. The cost of revitalization and equipping of well in the proposed exploration area for the purposes of thermal energy storage is estimated based on data on well depth, lithology, pressure and temperature conditions, and the duration of well equipping including well testing. BTES wells also require special well equipping by inserting specialized vacuum insulated tubing to exchange heat. The price also includes the cost of services, equipment and materials based on current well construction prices in 2025. The length of the well channel was also taken into account when analyzing the well price.

Table 12. Projected main capital expenses for Savica-1 well

Projected Main Capital Expenses	
Documentation	
- Preparation documentation of the work program for the intervention	20.000 €
- Technical documentation (Concept and Main Elaborate of proven heat reserves, Production and Reservoir engineering elaborate, Environmental impact study)	200.000 €
Land purchasing and preparatory construction work	
-Land purchasing for construction area and workover rig operations	50.000
- Preparation of the work site 30 x 30 m and construction of an access road	300.000 €
Well workover operations	
- Mobilization and installation of the workover rig	125.000 €
- Mounting of the completley new wellhead and preventer system	100.000 €
- Cleaning operations of cased hole and open hole with survey and logging	250.000 €
- Isolated specalized tubing for heat exchange - 600 m of 7" L80 23Lb x 5 1/2" L80 17lb Aerogel+Composite Insulated Casing with BTC Connections Range 2 - 1600 m 5 1/2" L80 12.75b x 3 7/8"" L80 6.5lb Aerogel+Composite Insulated Tubing with BTC Connections Range 2	90.000 € (150 €/m) 176.000 € (110 €/m)
- Installation of production equipment - DBHE	300.000 €
- Hermeticity testing and flow testing	50.000 €
Mechanical work	
- Assembly of surface equipment for heat production (surface installations and fittings, installation of heat exchanger, construction of power plant pipeline, installation of pumps)	300.000 €
Electrical works	
- Installation of electrical equipment and control system	100.000 €
- Connection to the local power grid	50.000 €
Pipeline	
- Waste heat pipeline from the power plant	500.000 €
-Pipeline to consumers	500.000 €
TOTAL INVESTMENT	3.111.000 €

The following assumptions must be defined for the economic and financial analysis for Savica-1 when actual investment takes place. The calculation must be made without indexing prices according to inflationary market trends. Since it is difficult to predict the future movement of energy prices on the revenue side, as well as on the expenditure side of the project, this factor could not be taken into account in the economic and financial assessment. The project should be analyzed over a period of 2 years for the exploration phase, followed by 3 years of construction and 25 years of production, amounting to a total of 30 years. Although the isothermal exploitation period of geothermal energy is not applicable for BTES as reservoir regenerates itself thermally due to storage of waste heat, 30 years is the time frame commonly used in energy project analyses in line with the guidelines of the European Commission's Cost-Benefit Analysis Guide (EC, 2014). The residual value of the investment after the analyzed period and depreciation should not be considered as a undepreciated part. However, given the market value of wells, facilities, and equipment, the remaining value after 25 years of production could be assessed differently, since these technological facilities can continue to be used for the same purpose with regular maintenance and overhauls. Therefore, the economic lifetime of the project is significantly longer than 25 years of exploitation. Decommissioning costs for well abandonment were not included in the calculation, as it is possible to continue using the wells even after 25 years of operation. Such costs may occur either before or after the 25-year period in the case of an unforeseen event or cessation of production. According to the European Commission's Cost-Benefit Analysis Guide (EC, 2014), a discount rate of 5% is typically recommended. Since the Savica-1 well is intended for revitalization and repurposing into a BTES system, with uncertainties related to technical reconstruction, storage performance and long-term operational conditions, the economic calculation should be carried out using a higher discount rate of 10%. Considering that there are previous results of exploratory drilling, but thermal energy storage has not been investigated at the location, it is possible to use a different discount rate than the one mentioned. For this reason, as part of the economic analysis, an NPV profile should be created for the technological variant at different discount rates of 1-20%. A rate of 5-7% is normally a common discount rate used in the segments of exploitation activities, while the use of a higher discount rate is associated with potential risks of geothermal potential research, but also changes in exploitation quantities, prices of capital costs and exploitation conditions. Since there is no production of fluids in this system, geological risks are relatively small compared to traditional hydrothermal energy systems. It is possible to take into account a higher discount rate in the initial phase of the potential assessment (12%) in order to amortize the geological risks if any, while after testing the well for extraction and rejection rates of heat it is possible to take into account a lower discount rate of 5-7% in the investment study. Exploitation fees, as defined by the Regulation on Fees for Hydrocarbons Exploration and Exploitation (OG 25/2020), Section IV – Fees for the exploitation of geothermal water, are not applicable in the case of the Savica-1 well. Since the well is planned for thermal storage and does not involve permanent abstraction of geothermal water, no concession procedure for exploitation of a geothermal aquifer is required. The project is therefore not subject to exploitation fees under the Hydrocarbons Exploration and Exploitation Act (OG 52/18, 52/19, 30/21). Nevertheless, this kind of system is still not recognized in Act, therefore model could be developed to pay certain concession related to amount of heat produced. For the revenue calculation, different heat energy prices must be taken into account. One reference value is the HEP heat energy price for industrial consumers, which is around 45 EUR/MWh. In the calculation, the heat energy price should be based on the average price of existing district heating distributors, reduced by certain amount of discount to attract demand. This reference price will depend on the demand of industrial consumers in the considered area, for district heating, agricultural (greenhouse) use or for other industrial applications, and which will also depend on direct negotiations with final consumers on site. The technological option involves the storage of thermal energy and the revitalization of the Savica-1 well. The option has been energy analyzed in detail, although there are various limitations that cannot be economically evaluated with high certainty at this moment. Namely, the limitations include resolving relations with the owners of the land on which the well working area is planned to be located. The technological option considers the relevant costs of land and the necessary documentation and the implementation of all necessary procedures that precede obtaining approval for exploration and energy storage and within the legal timeframe required for their acquisition. The project completion time may be several times longer, and the costs of individual

contributions (municipal and water management) may be extremely high, which may negatively affect the project results, but the exact amount cannot be predicted at this moment, so they need to be considered as unforeseen costs amounting to 2% of the investment costs in each year of investment.

The planned revenues from the sale of thermal energy are offset by the costs of internal energy consumption required for system operation, including circulation pumps for the borehole heat exchanger (BHE) and the possible heat pumps, as well as other operating expenses. Energy costs must be estimated based on the expected pump work, injection and extraction heat level conditions, and the electricity demand of the heat pumps. These costs are estimated by the efficiency factor SPF, defined as the ratio of heating energy delivered by the heat pump annually to that of the total compressor power required by the heat pump annually.

Maintenance costs should be estimated at approximately 3% of annual revenues from thermal energy use. Personnel costs should be calculated on the basis of an annual gross salary for an operating technician.

8.2. Defining Project Risks

Project risk definition includes the following essential activities:

- identification of risks,
- conducting a qualitative risk analysis,
- monitoring,
- conducting a quantitative risk analysis.

As part of the investment study, potential risks should be identified and a qualitative risk analysis should be conducted. In the next step of the project, during the preparation of the investment study, when all critical variables and their impact on the financial and economic outcomes of the project will be known, it will be necessary to carry out a sensitivity analysis of the project considering the variation of individual critical variables and carry out a quantitative risk analysis. The following section presents a qualitative risk analysis, taking into account the main technical-technological, economic, environmental, and institutional barriers that may realistically occur during the project and affect, to a greater or lesser extent, the realization of the project itself or its results. During the risk analysis, it is necessary to define critical variables, their probability, their impact, and the overall level of risk (probability × impact), along with proposed measures for risk prevention and mitigation in case risks occur. The risk analysis methodology should be carried out according to the risk gradation system of probability (Guide to Cost-Benefit Analysis of Investment Projects 2014–2020, European Commission, 2014) and is presented in Table 12. The probability of risks should be assessed on a scale of 0–100% across five levels of likelihood (0–10% very unlikely, 10–33% unlikely, 33–66% neither likely nor unlikely, 66–90% likely, 90–100% very likely). Impact should be assessed across five categories (1 – not relevant, 2 – minor impact, 3 – moderate impact, 4 – critical impact, 5 – catastrophic impact). The overall risk level must be evaluated as low, moderate, high, or very high.

PROBABILI	IMPACT					
		1 – not relevant	1 – not relevant	3 – moderate impact	4 – critical impact	5 – catastrophic impact
	0–10% very unlikely	Low	Low	Low	Low	Moderate
	10–33% unlikely	Low	Low	Moderate	Moderate	High

T Y	33–66% neither likely nor unlikely	Very low	Moderate	Moderate	High	High
	66–90% likely	Very low	Moderate	High	Very high	Very high
	90–100% very likely	Moderate	High	Very high	Very high	Very high

Table 13. Risk gradation according to probability and impact (Guide to Cost–Benefit Analysis of Investment Projects 2014–2020, European Commission, 2014)

For each identified risk, it is necessary to describe the cause of the risk, the consequences, and the impact on costs, benefits, project implementation time, and financial sustainability. It is also essential to specify the risk owner, how the risk can be influenced, and the project phase in which the risk occurs (preparatory phase, implementation phase, or operational period).

All impacts on financial indicators will need to be examined as part of the preparation of the investment study and sensitivity analysis. Possible project risks are presented in Table 13, while the qualitative analysis during project implementation is presented in Table 14.

1. Technical and technological risks
Risk of inability to realize the proposed technological option at the site
Risk of deviation from expected stored or retrieved thermal energy
1. Economic risks
Change in the amount of investment
Change in annual operating costs
Risk of energy price changes
2. Environmental risks
Construction restrictions due to environmental impacts and spatial planning restrictions
Accidental situations
Risk of ecological accident
Risks of pollution after the end of system operation
3. Institutional risks
Inability to secure conditions for construction in the designated area
Lengthy process of obtaining exploitation permits
Changes in purchase prices of thermal energy/waste heat
4. Global risks
Risk of interruption of supply chains and inability to procure equipment, materials and raw materials as a result of geopolitical events in the world
Extreme fluctuations in energy and raw material prices due to global geopolitical events

Table 14. Possible risks of the BTES project at the Savica-1 well

1. TECHNICAL–TECHNOLOGICAL RISKS				
RISK	P	I	P×I	DESCRIPTION AND MITIGATION MEASURES
Risk of inability to realize the proposed technological option at the site				Risks are present due to revitalization risks (cleaning of the well, cement/casing stability) and general technological risks (design of technological equipment). The risk of impossibility of technological implementation at the location is possible due to for example the population density, but also the usability of free space. When locating the wells, it is necessary to secure land for the location of the well working area.
Risk of deviation from expected stored or extracted thermal energy				The risk of change in expected energy yield is possible and very high, with the consequences of this risk potentially having a significant impact on the realization of the project and on the results of the project itself.
2. ECONOMIC RISKS				
Risk	P	I	P×I	DESCRIPTION AND MITIGATION MEASURES
Change in the amount of investment and change in annual operating costs				The change in the amount of investment as well as the change in the amount of annual operating costs is very likely, it is only a matter of the amount of that change. At this stage, without knowing the final capacity of the deposit, the final selection of the project's technological solution, and understanding the operation of the facility as well as identifying potential consumers, it is impossible to estimate all the financial inputs that should affect the financial structure of investment and operating costs. For example, the contractors for certain works are not known, so the cost of performing them is also unknown if done by a specific participant in the project. Namely, these costs have been estimated based on the services provided by service companies in this field, but there are service companies in this market that have the logistics and infrastructure to carry out a large part of the aforementioned technical and technological works required for the construction and equipping of wells for extraction or the construction of other surface infrastructure.

				On the other hand, the investor can apply as an entity that is qualified to apply for various projects within the EU for the withdrawal of funds with the aim of increasing the share of renewable energy sources and energy transition. Certain investment costs related to the construction and equipping of new wells for geothermal energy exploitation will be able to be estimated more accurately after the initial works and testing in new wells. Likewise, operating costs will be able to be estimated after selecting the exact microlocation of the well working area and heat exchangers for individual final consumers, although they will still be extremely sensitive to changes in energy prices, as will project revenues.
Risk of energy price changes				The economic risks of the project include the risk of changes in energy prices. Currently, reference values for the market price of thermal energy are not known. Changes in energy prices need to be taken into account, although it is not possible at this moment to predict future price movements; therefore, a sensitivity analysis on changes in electricity prices has been conducted. Based on historical price movements of energy as well as geopolitical trends in the upcoming period, it is possible to expect prices to remain at similar levels for gas, oil, and thermal energy. Changes in energy prices can affect both the revenue and expenditure sides of the project. Revenues are calculated based on predicted prices for thermal energy, while expenditures are calculated based on annual operational costs for the energy needs of pump operation and heat pumps consumption
3. ENVIRONMENTAL RISKS				
Construction restrictions due to environmental impacts and spatial planning restrictions				Well is not in the protected area
Accidental situations and risk of ecological accident				In the event that an accidental situation occurs during the execution of the observed procedure, there will be a heat exchange with the external atmosphere. According to the available analyses of the chemical composition of the water, the production of gasified water is not expected, but it is not excluded. In that case, it is necessary to carry out technical interventions and remediate the problem and prevent the leakage of water into the environment. However, it is necessary to analyze the adverse impacts on the environment considering the composition and quality of the water. It is necessary to analyze the penetration of water into the soil and/or on the surface due to corrosion of transport pipelines, taking into account the mineral

				composition in order to define the level of risk, i.e. whether the hot water poses a danger to any component of the environment.
Risks of pollution after the end of system operation				If the use of geothermal energy ceases, wells must be sealed or properly abandoned to ensure system integrity. Surface structures will be removed, and works may cause temporary dust emissions, but with no long-term impacts. Well abandonment will follow industry standards. Technical documentation and site-specific conditions must be considered, including cement plugs at adequate depths, removal of casing heads, and welding of protective covers. Soil restoration and agricultural measures must return the site to its original condition.
4. INSTITUTIONAL RISKS				
Inability to secure conditions for construction in the designated area				
Risks related to obtaining permits and documentation				The lengthy process of obtaining permits for geothermal energy exploitation represents a real risk. Due to the complexity of legal requirements, which demand extensive procedures for securing all necessary documentation (exploitation decision, mining projects, environmental impact study, location and building permits for wells and installations), delays in project implementation are possible. Risks can be minimized through clear project management, cooperation with the competent Ministry and Hydrocarbon Agency, and by establishing transparent and straightforward processes. Defining the obligations of project participants and clarifying the roles of stakeholders, including local authorities and end users, is key to minimizing such risks.
Changes in purchase prices of thermal energy				Changes in the reference price of thermal energy have a very high impact, with a 90% probability of occurrence, meaning that the financial viability of the project depends directly on stable pricing. To mitigate this risk, it is important to base project revenues on available price levels from HEP Toplinarstvo, with a reduction of around 30% applied to ensure competitiveness in comparison with other heat energy sources.
5. GLOBAL RISKS				
Risk of supply chain disruptions and inability to procure equipment,				The risk of supply chain disruptions and inability to procure equipment, materials, and raw materials due to geopolitical developments is currently assessed as moderate, since no significant disruptions in supply chains of raw materials and energy are present at the time of preparing this study.

materials, and raw materials due to geopolitical developments worldwide				However, such impacts could occur in all procurement segments. It is assumed that the situation will remain relatively stable during project implementation, provided there are no major geopolitical changes on the global or regional market.
Extreme fluctuations in energy and raw material prices due to geopolitical developments worldwide				Extreme fluctuations in energy and raw material prices due to geopolitical developments worldwide are considered highly likely at the time of preparing this study, despite the relatively stable global market. Although no significant disruptions in energy markets are currently present, such impacts could occur if major geopolitical changes take place at the global or regional level. These disruptions could be extreme and have a critical influence on the project and thus cannot be ignored.

Table 15. Qualitative risk analysis during project implementation

9. Conclusion

This Study presents integral modelling of surface equipment and subsurface reservoir for the utilization of a Deep geothermal Borehole Heat Exchanger (DBHE) for the Savica-1 case study (located in City of Zagreb, Croatia). The conceptual model is presented with main equations, and the geothermal reservoir is modelled in external software FeFlow. A total of four configurations have been tested with differences in length and diameter of the casing and whether reheating is included or not. All four tested cases showed different annual energy flows, indicating the need for a-priori testing as presented in this paper. Longer tubing leads to higher hydraulic losses and higher power consumption, but reduces the need for the waste heat, which is favorable if waste heat comes at high cost. Also, longer tubing can reach higher temperatures and can provide a higher amount of direct heating. The influence of BTES is seen at the higher heat supply from the waste heat for reheating and higher supply of direct heating from the geothermal for district heating supply. Future work or direct investment at this site should be focused on integration of renewable power into the system to make the heating fully 100% renewable and carbon-free.

10. References

1. Basch, O. (1983): Basic Geological Map 1:100 000. Explanatory notes for sheet Ivanić-Grad L 33-81. Geološki zavod Zagreb (1980), Savezni geološki zavod Beograd (in Croatian).
2. Diersch, H-J. G. (2014). FEFLOW – Finite Element Modeling of Flow, Mass and Heat Transport in Porous and Fractured Media. Springer Verlag Berlin Heidelberg. ISBN 978-3-642-38739-5.
3. HOPS – Croatian Transmission System Operator Ltd. (2022): Ten-Year Transmission Network Development Plan 2023–2032, with detailed elaboration for the initial three-year and one-year period. HOPS, Zagreb, Croatia.
4. Jelić, K. (1979). Termičke osobine sedimentacionog kompleksa jugozapadnog dijela Panonskog bazena [Thermal properties of the sedimentary complex in the southwestern part of the Pannonian Basin]. Doctoral dissertation, Faculty of Mining, Geology and Petroleum Engineering, University of Zagreb, Zagreb. (in Croatian).
5. Jelić, K. (1984). Odnos gustoće i poroznosti s dubinom litostratigrafskih formacija Savske i Dravske potoline [Relationship of density and porosity with depth in lithostratigraphic formations of the Sava and Drava depressions]. Nafta, 35(12), Zagreb. (in Croatian).
6. Jelić, K. (1987). Stacionarna geotermijska energija u Savskoj i Dravskoj potolini Panonskog bazena SR Hrvatske. Nafta.
7. Lund, H., Werner, S., Wiltshire, R., Svendsen, S., Thorsen, J. E., Hvelplund, F., & Mathiesen, B. V. (2014). 4th Generation District Heating (4GDH) – Integrating smart thermal grids into future sustainable energy systems. Energy, 68, 1–11. https://doi.org/10.1016/j.energy.2014.02.089
8. Magyar, I., Geary, D. H., & Müller, P. (1999). Paleogeographic evolution of the Late Miocene Lake Pannon in Central Europe. Palaeogeography, Palaeoclimatology, Palaeoecology, 147(3–4), 151–167. https://doi.org/10.1016/S0031-0182(98)00155-2
9. Malvić, T. (2016). Regional turbidites and turbiditic environments developed during Neogene and Quaternary in Croatia. Materials and Geoenvironment, 63(1), 39–54. https://doi.org/10.1515/rmzmag-2016-0004
10. Malvić, T.and Velić, J. (2011). Neogene tectonics in Croatian part of the Pannonian Basin and reflectance in hydrocarbon accumulations. In: Schattner, U. (Ed.), New Frontiers in Tectonic Research: At the Midst of Plate Convergence. InTech, Rijeka, pp. 215–238. https://doi.org/10.5772/21270
11. Podbojec, M., and Cvetković, M. (2015). Preliminary estimate of CO_2 storage capacity by petrophysical modelling in Upper Miocene Poljana Sandstones in the western part of the Sava Depression. Rudarsko-geološko-naftni zbornik, 31(1), 31–43. https://doi.org/10.17794/rgn.2016.1.3
12. Royden, L. H. (1988). Late Cenozoic tectonics of the Pannonian Basin System. AAPG Memoir 45, AAPG, Tulsa, pp. 27–48.

13. Velić, J., Weisser, M., Saftić, B., Vrbanac, B., & Ivković, Ž. (2002). Petroleum-geological characteristics and exploration level of the three Neogene depositional megacycles in the Croatian part of the Pannonian Basin. Nafta: Exploration, Production, Processing, Petrochemistry, 53(6–7), 239–249.
14. Vrbanac, B., Velić, J., & Malvić, T. (2010). Sedimentation of deep-water turbidites in the SW part of the Pannonian Basin. Geologica Carpathica, 61(1), 55–69. https://doi.org/10.2478/v10096-010-0001-8